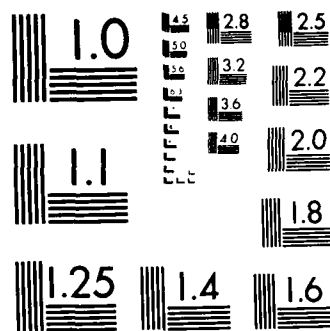


FUELS COMBUSTION RESEARCH(U) PRINCETON UNIV NJ DEPT OF MECHANICAL AND AEROSPACE ENGINEERING F L DRYER ET AL. 31 OCT 86 AFOSR-TR-86-2107 F49620-86-C-0006 171

F/G 21/2

Nil



MICROCOPY RESOLUTION TEST CHART  
NATIONAL BUREAU OF STANDARDS-1963 A

REPORT DOCUMENTATION PAGE

AD-A175 040

DTIC  
S  
REF ID: A175040  
DEC 1 2 1986

1b. RESTRICTIVE MARKINGS None		
3. DISTRIBUTION/AVAILABILITY OF REPORT Distribution unlimited; approved for public release		
5. MONITORING ORGANIZATION REPORT NUMBER(S) <b>AFOSR-TR- 86-2107</b>		
2b. DECLASSIFICATION/DOWNGRADING SCHEDULE	4. PERFORMING ORGANIZATION REPORT NUMBER(S)	7a. NAME OF MONITORING ORGANIZATION Air Force Office of Scientific Research
6a. NAME OF PERFORMING ORGANIZATION Princeton University	8a. OFFICE SYMBOL (If applicable)	7b. ADDRESS (City, State and ZIP Code) Bolling AFB DC 20332-6448
6c. ADDRESS (City, State and ZIP Code) Dept. of Mech. and Aero. Eng. Princeton, NJ 08544	8b. OFFICE SYMBOL (If applicable) AFOSR/NA	9. PROCUREMENT INSTRUMENT IDENTIFICATION NUMBER F49620-86-C-0006
6a. NAME OF FUNDING/SPONSORING ORGANIZATION Air Force Office of Sci. Res.	8c. ADDRESS (City, State and ZIP Code) Bolling AFB DC 20332-6448	10. SOURCE OF FUNDING NOS.
		PROGRAM ELEMENT NO. 61102F
		PROJECT NO. 2308
		TASK NO. A2
		WORK UNIT NO.
11. TITLE (Include Security Classification) Fuels Combustion Research		
12. PERSONAL AUTHOR(S) F.L. Dryer, I. Glassman, and F.A. Williams		
13a. TYPE OF REPORT Annual	13b. TIME COVERED FROM 1Oct85 to 30Sep86	14. DATE OF REPORT (Yr., Mo., Day) 1986 Oct. 31
15. PAGE COUNT 58		
16. SUPPLEMENTARY NOTATION		
17. COSATI CODES		
FIELD	GROUP	SUB. GR.
21	01	
21	02	
18. SUBJECT TERMS (Continue on reverse if necessary and identify by block number)		
Soot formation Boron Cloud Combustion		
Aromatic Fuel Oxidation		
Boron Slurry Combustion		
19. ABSTRACT (Continue on reverse if necessary and identify by block number)		
<p>After great progress related to soot formation in normal diffusion flames, studies of near sooting inverse diffusion flames were begun to determine controlling precursors. Stable, temperature controlled inverse diffusion flames have been successfully developed and numerous chemical samples extracted and analyzed. Observed trends are being studied.</p> <p>The side chain oxidation of n-butyl benzene was found to follow the same processes as the smaller n-alkyl benzenes; abstraction, alkyl group displacement and thermal cleavage. The results have led to development of a simple general, mechanistic model for the oxidation of n-alkyl benzenes.</p> <p>Combustion property observations of isolated boron droplets were extended to boron/JP-10 slurries with various solid loadings. Some physical understanding of observed droplet-burning and disruption behavior was developed. Quasi-spherical hollow shells of the boron agglomerate with blowholes support the hypothesis of the formation of the impermeable shell and subsequent disruption of the primary slurry droplet. (continued)</p>		
20. DISTRIBUTION/AVAILABILITY OF ABSTRACT		
UNCLASSIFIED/UNLIMITED <input checked="" type="checkbox"/> SAME AS RPT. <input type="checkbox"/> DTIC USERS <input type="checkbox"/>		
21. ABSTRACT SECURITY CLASSIFICATION Unclassified		
22a. NAME OF RESPONSIBLE INDIVIDUAL Julian M. Tishkoff	22b. TELEPHONE NUMBER (Include Area Code) (202)767-4935	22c. OFFICE SYMBOL AFOSR/NA

NOT FILE COPY

Boron suspension (cloud) combustion in the hot reaction products of a flat-flame burner has been pursued. The boric acid fluctuation bands were identified spectroscopically, and conditions for their flame occurrence measured. The work progresses toward establishment of ignition conditions and combustion times of 0.1-5 micron boron particles.



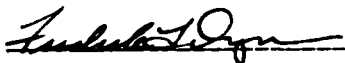
Accession For	
NTIS CRA&I	<input checked="" type="checkbox"/>
DTIC TAB	<input type="checkbox"/>
Unannounced	<input type="checkbox"/>
Justification	
By	
Distribution/	
Availability Codes	
Dist	Avail and/or Special
A-1	

**AFOSR-TR. 86-2107**

**AFOSR 86-C-0006**

**Annual Technical Report Under AFOSR Contract  
F49620-86-C-0006  
Air Force Systems Command  
Air Force Office of Scientific Research**

**FUELS COMBUSTION RESEARCH**



**Frederick L. Dryer  
Professor  
Principal Investigator**



**Irvin Glassman  
Professor  
Principal Investigator  
Correspondent**



**Forman A. Williams  
Professor  
Principal Investigator**

**Approved for public release;  
distribution unlimited.**

**School of Engineering and Applied Science  
Department of Mechanical and Aerospace Engineering  
PRINCETON UNIVERSITY  
Princeton, New Jersey 08544**

**October 31, 1986**

## TABLE OF CONTENTS

	<u>Page No.</u>
Summary .....	1
I. Research Objectives .....	2
II. Status of the Research and Year's Progress .....	3
A. Pyrolysis and Oxidation of Aromatic Fuels .....	3
B. Soot Formation and Destruction Process .....	12
C. High Energy Density (Boron) Slurry Vaporization/ Combustion Processes .....	18
1. Free Slurry Droplet Combustion .....	18
2. Boron Suspension (Cloud) Combustion .....	23
References .....	28
Table 1 .....	30
Table 2 .....	32
Table 3 .....	33
Figure Captions .....	34
Figures .....	36
III. Publications Related to Current Effort .....	52
IV. Professional Personnel and Graduate Students Theses ....	56
V. Presentations - Seminars .....	57
VI. Interaction with Other Laboratories .....	58

## SUMMARY

After great progress related to soot formation in normal diffusion flames, studies of near sooting inverse diffusion flames were begun to determine controlling precursors. Stable, temperature controlled inverse diffusion flames have been successfully developed and numerous chemical samples extracted and analyzed. Observed trends are being studied.

The side chain oxidation of n-butyl benzene was found to follow the same processes as the smaller n-alkyl benzenes: abstraction, alkyl group displacement and thermal cleavage. The results have led to development of a simple general, mechanistic model for the oxidation of n-alkyl benzenes.

Combustion property observations of isolated boron droplets were extended to boron/JP-10 slurries with various solid loadings. Some physical understanding of observed droplet-burning and disruption behavior was developed. Quasi-spherical hollow shells of the boron agglomerate with blowholes support the hypothesis of the formation of the impermeable shell and subsequent disruption of the primary slurry droplet.

Boron suspension (cloud) combustion in the hot reaction products of a flat-flame burner has been pursued. The boric acid fluctuation bands were identified spectroscopically, and conditions for their flame occurrence measured. The work progresses toward establishment of ignition conditions and combustion times of 0.1-5 micron boron particles.

### I. Research Objectives

Present and anticipated variations in fuels and trends toward high performance propellants require greater understanding of the chemical phenomena associated with the combustion aspects of the various propulsion systems of current and future interest to the Air Force. Under AFOSR an integrated,

fundamental program on fuel research was established at Princeton. Current emphasis and research objectives are directed towards understanding soot formation and destruction processes; on related pyrolysis and oxidation studies of hydrocarbons, particularly the various types of aromatics that aggravate soot conditions and are the components of heavy fuels, and mastering high energy density boron and slurry combustion problems.

In subsequent sections this report details the progress made during the past year and the publications which have emanated from the work.

## II. Status of the Research and Year's Progress

This section is divided into three parts which correspond to the current major objectives of the research program.

### A. Pyrolysis and Oxidation of Aromatic Fuels

Previous investigations (1-3) of the high temperature (1000-1200K) oxidation of methyl, ethyl and n-propyl benzene in the Princeton flow reactor have indicated that three primary processes are instrumental in removing the alkyl side chain from the aromatic ring: 1) abstraction of a hydrogen from the alkyl group, decomposition of the radical and, oxidation of the subsequently formed species; 2) displacement of the alkyl group by a radical species—usually an H atom; 3) thermal cleavage (homolysis) of part of the side chain followed by oxidation of the resultant radicals. Since the side chain is removed initially by these three processes without any major attack on the aromatic ring (4,5), it was also found that the oxidation of alkylated aromatics eventually reduces simply to the oxidation of the phenyl radical and/or benzene. Much of the basic understanding of the reactions important in the removal of the side chain was gained from observing that the chemistry of the oxidation of methyl, ethyl and n-propyl benzene was analogous in many ways to the oxidation chemistry of methane



(6), ethane (7) and propane (7,8).

In order to examine if the same three processes of abstraction, displacement and homolysis found previously would also be responsible for the removal of the larger and possibly more complex, n-butyl side chain, a high temperature oxidation study was conducted of n-butyl benzene, another member of the homologous series. The study was also undertaken in order to establish if the oxidation chemistry of n-butane (9), the corresponding next member of the analogous n-alkane series, would serve as a guide in the understanding of the details of the reactions of the n-butyl side chain.

Recently acquired n-butyl benzene flow reactor oxidation data are presented which confirm that the same three processes are again responsible for the removal of the side chain and that the oxidation of n-butane is indeed a good indicator of important side chain reactions. In addition, the understanding gained from the study of the oxidation of n-butyl benzene along with that acquired in previous oxidation studies of the smaller members of the homologous series has lead naturally to the development of the generalized model of the high temperature oxidation of n-alkyl aromatics presented later.

The major species profiles and auxiliary information obtained from the rich oxidation of n-butyl benzene are displayed in Figures 1-4. Similar profiles were obtained from both lean and stoichiometric oxidation experiments.

Figure 1 indicates the rapid decay of the fuel is an apparently first order process. The exponential decay of the fuel is more clearly indicated in the semi-log plot of the fuel decay profile displayed in Figure 5. A highly correlated straight line fit to the n-butyl benzene profile is obtained over two orders of magnitude decrease in concentration. An apparent first order decay of fuel during an oxidation experiment has been demonstrated (2,10) to imply a

quasi-steady concentration of the free radical pool.

A few points about the various species profiles should be noticed. By far the largest concentration of early forming intermediates is ethylene. During the same time period that the ethylene is growing toward its maximum concentration, styrene and toluene are growing toward their maxima. Ethyl benzene, propenyl benzene and propene appear to reach maxima somewhat earlier than do the other intermediates. Though the relative sequence of maxima in concentrations do not directly indicate the order of formation of species and their causal relationships, they can nevertheless be suggestive of mechanistic paths to be examined.

The growth profile of benzaldehyde and the comparatively late maxima in the concentration profiles of benzene and phenol are characteristic of the oxidation of alkyl aromatics (5). A number of trace quantities of other species primarily characteristic of the decomposition of the aromatic ring (4,5) were detected but have not been plotted.  $\text{CO}_2$  formation was not measured during the experiment. Judging from the quantity of CO produced however, the expected amount of  $\text{CO}_2$  would be extremely low.

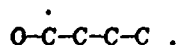
The experimental results displayed in Figures 1-4 can serve as a test of the viability of extending previously developed mechanistic ideas to larger n-alkyl aromatics. The measure of the success of the extension will be the degree to which the presence of the observed intermediates is predicted when the mechanistic principles are applied to the new fuel. Thus the application of previously developed principles to the oxidation of n-butyl benzene is examined; the contribution of each mechanistic path to the observed aromatic intermediate species is particularly noted.

The three side chain removal pathways broadly denoted as abstraction,

displacement and homolysis are again postulated to be the major routes by which the n-alkyl group is removed from the alkylated aromatic. Though these three types of reaction sequences were found to be common to the oxidation of methyl, ethyl and n-propyl benzene, their relative significance varied with the nature of the side chain. Thus, the mechanistic details of the three routes as applied to n-butyl benzene will be similar to those found previously but will differ in amount of detail and degree of significance. For convenience, a summary of the n-butyl benzene reactions that are described in the following paragraphs along with the analogous reactions of n-butane that aided in their selection is presented in Table 1.

N-butyl benzene differs from its predecessors in the homologous series in that it offers a greater number of side chain abstraction sites. The n-butyl side chain contains 2 benzylic, 3 primary and 4 secondary hydrogens. The four secondary hydrogens are in turn comprised of 2 sets of mechanistically distinct sites. Though there is selectivity associated with the abstraction of each type of hydrogen, reaction path degeneracy prevents the predominance of reaction at any one site for the oxidation of alkylated benzenes at the present conditions (10,11). Therefore, the production of intermediates by abstraction of a hydrogen at each site by a pool composed of the most active radicals, OH, H and O, must be individually evaluated.

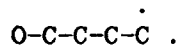
The benzylic C-H bond is the weakest in the side chain (12). Abstraction of an H from this site produces the radical



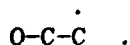
A unimolecular beta scission process, the dominant high temperature radical decomposition process at flow reactor conditions, contributes to the experimentally observed concentration of styrene. The process also produces ethyl

radicals which at these conditions forms ethylene and H through a unimolecular decomposition (2).

Abstraction of any one of the three primary H atoms forms a radical of the type

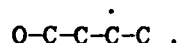


Examination of the structure of this radical indicates that beta scission yields ethylene and the 1-phenyl-2-ethyl radical



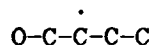
The thermodynamically favored path for beta scission of this radical is the loss of the benzylic H which further contributes to the observed concentration of styrene.

Removal of a secondary hydrogen from the third carbon of the side chain leads to the formation of

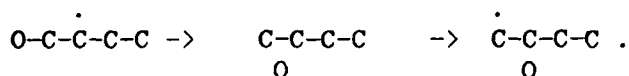


The beta scission bond breaking process of this radical is also predictable; it contributes to the relatively large amount of propylene that was observed and produces a benzyl radical. The benzyl radical cannot undergo beta scission because no beta carbon-carbon bonds exist. However, three alternate reaction routes are probable. Oxidation through reaction with O and HO<sub>2</sub> (1) contributes to the observed concentration of benzaldehyde. Radical-radical reaction with methyl, highly probable because of the long lived nature of both the methyl and benzyl, undoubtedly contributes to the large concentration of ethyl benzene (3,11). Reaction of the benzyl radical with a suitable H source yields a portion of the observed toluene.

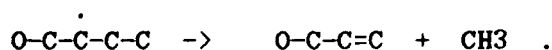
Abstraction of a hydrogen from the set of secondary H atoms on the second carbon of the side chain presents an interesting test of the phenyl isomerization process found to be surprisingly important during the oxidation of n-propyl benzene (3). The 1-phenyl-2-butyl radical formed by the abstraction



can be converted to the 2-phenyl-1-butyl radical through the following sequence (3,13)



Beta scission of the 2-phenyl-1-butyl radical would provide another source of styrene and ethylene (via decomposition of ethyl radical). In competition with the above isomerization is the beta scission of a C-C bond in the initially formed 1-phenyl-2-butyl radical to yield propenyl benzene and methyl radical:



The observed propenyl benzene concentrations are of the order of magnitude of the other early forming intermediates suggesting that the beta scission process is at least as important as the phenyl isomerization route. Since styrene formed through the isomerization path cannot be distinguished in the current experiments from that formed through other paths, the extent of isomerization can not be experimentally evaluated.

The products observed during the oxidation of n-propyl benzene led to the conclusion, unlike that described above, that the phenyl isomerization was the dominant path for the secondary phenyl propyl radical. The dominance of the isomerization route was due in large part to the absence of any beta C-C bonds in

the side chain, a situation not repeated for the secondary phenyl butyl radical.

Displacement of the alkyl side chain is well known for toluene (14) and has been demonstrated for ethyl and n-propyl benzene (2,3). Displacement by an H atom of the n-butyl side chain contributes to the observed benzene and also produces an n-butyl radical. The mechanism for the oxidation of n-butane (9) suggests that the n-butyl radical will primarily undergo beta scission to form ethylene and an ethyl radical which itself contributes further to the concentration of ethylene.

Larger alkylated aromatics such as n-butyl benzene offer a number of possible sites for thermal C-C cleavage. The bond between the benzylic carbon and the second carbon atom of the chain is the weakest (12). At the conditions of the current experiments bond breaking would be predicted to occur at this site forming benzyl and n-propyl radicals. The following argument illustrates the reasoning behind this prediction. The homolysis of n-butyl benzene at the benzylic site should have high pressure Arrhenius parameters of  $A=10^{15.3}\text{sec}^{-1}$  and  $E=70\text{Kcal}$  if the trend demonstrated in studies of ethyl benzene (15) and n-propyl benzene (16) holds. Homolysis at the bond site between the second and third carbon would be expected to take place without any influence from the beta position phenyl ring (17). Therefore a representative high pressure Arrhenius rate expression of  $k=10^{16.3}\exp-(81\text{Kcal}/RT)\text{sec}^{-1}$  corresponding to the central bond scission of butane (9) can be taken for the analogous reaction of n-butyl benzene. Evaluation of the two rate expressions at 1000K indicates that homolysis at the benzylic site is more than an order of magnitude faster than at the 2-3 bond site.

The fate of benzyl radicals that are produced from the major homolysis path is the same as was discussed earlier. The major decomposition path for n-propyl is beta scission to form more ethylene and a methyl radical (8).

The reaction paths described above rationalize quite well the early production of styrene, propenyl benzene, toluene, benzaldehyde, ethyl benzene and benzene. The many reaction paths that form both styrene and ethylene are consistent with the large amounts of these species formed very early. The large amount of ethylene, early toluene formation and some benzaldehyde production are also consistent with further oxidation of styrene (2) as well as with the other enumerated sources.

During the oxidation of the other members of the homologous series, the same aromatic intermediates, styrene, toluene, ethyl benzene, benzaldehyde, phenol and benzene, were observed though in varying concentrations depending on the size of the side chain in the initial fuel. As was discussed earlier, the same basic mechanistic routes appeared to be responsible for the formation of these common intermediates. The observation that common species are produced through common paths from the oxidation of members of an homologous series strongly suggests that the construction of a generalized model of the oxidation process is possible.

A simple, generalized, mechanistic model for the oxidation of n-alkylated aromatics at temperatures in the vicinity of 1000K and at 1 atmosphere pressure that attempts to represent the major steps by which the alkyl side chain is removed from the aromatic ring is presented schematically in Figure 6. The three main fuel consumption routes of displacement, abstraction and homolysis are clearly displayed. The key species responsible for the formation of the observed intermediates are also displayed. The arrows in the figure represent the causal relationships that convert one species to another. Included but not explicitly noted as such, is the oxidative chemistry that transforms one set of intermediates into the next. The vertical arrows originating at styrenes (a term

meant to represent styrene and all its substituted variations) and the arrows leading to phenyl imply the inclusion of oxidative paths such as those that produce benzaldehyde.

The formation of the intermediates ethyl benzene and propenyl benzene do not fall neatly into the generalized mechanism of Figure 6. However, the mechanism does indirectly encompass the chemistry of both of these species since each of these intermediates is itself a fuel that will undergo the same three basic processes of displacement, abstraction and homolysis. Therefore, when these intermediates are formed they can be considered to re-enter the scheme at the beginning "fuel" step.

Though the general mechanistic model of Figure 6 is predictive and expected to apply to alkylated aromatics such as n-pentyl and n-hexyl benzene, it is nevertheless qualitative. A simple quantitative mechanistic model for the oxidation of all n-alkyl aromatics would be useful for inclusion in a large computer code that describes a physical situation of which the chemistry is only one part. Though techniques exist (18) that can be used to make the present model quantitative, to do so would require rate constants representative of each pathway over an appropriate temperature and pressure range. At this time, such rate expressions are not available.

Two additional points need to be considered if a quantitative overall model to account for the oxidation of all mono-substituted monocyclic aromatics is to be developed. As the side chain gets longer, the number of olefins similar to propenyl benzene will somewhat increase. Though it is true that the chemistry of these species is qualitatively well accounted for by the present model, a means of quantitatively accounting for the increase in number with chain length would be required. Secondly, as the chain increases in length, the possibility of alkyl



side chain radical isomerizations with 5 and 6 member cyclic transition state increases. These type of isomerizations are well documented (19) for long chain alkyl radicals and can compete with rapid beta scission of initially formed radical. Isomerizations of this type will alter the proportion of the intermediate concentrations; primary or secondary radicals will tend to be converted to benzylic radicals with a consequent change in the stable species observed.

During the subject period work began, as well, on the oxidation di-alkylated aromatics. The initial results on xylene, a prominent component of jet propulsion fuels, looks most promising. A typical flow reactor result is shown in Fig. 7. Obviously more work is necessary before substantive conclusions or mechanisms can be given. This aspect of the research will be the main concern of the next annual report in this area. Indeed the DOD equipment grant through AFOSR leads us to expect that chemical analysis of the complex intermediates to be found in the flow reactor experimental tests on the alkylated and polynuclear aromatics will not be too difficult.

#### B. Soot Formation and Destruction Process

Extensive progress and understanding of soot processes have developed from this aspect of the AFOSR program. The program was the first to clearly distinguish the difference between sooting tendencies of pre-mixed and diffusion controlled combustion processes and the importance of considering temperature in analyzing the sooting tendency of fuels (20). The work on pre-mixed flames was completed and a correlation developed between the critical sooting equivalence ratio of fuels and mixtures and a single property of the fuel, namely the "number of C-C bonds" (21). Work on diffusion flames also has largely been completed. The importance of temperature was particularly significant for this type of

combustion process. The results of the program make it possible to determine from a fundamental knowledge of the pyrolysis kinetics of component fuels, their tendency to soot under diffusion flame conditions (22,23).

The key to controlling soot formation irrespective of controlling the temperature is a knowledge of the mechanism of soot formation, but perhaps, as important, the precursors that control the soot formation process. Thus for this annual period most attention was directed towards this objective by chemical sampling "unique" inverse diffusion flames and making use of the chemical instrumentation available in the oxidation kinetics aspect of the program. The sampling for these flames is performed at a near sooting condition which is developed by nitrogen dilution of the flame (20).

All hydrocarbon fuel, except methane, tend to form so much soot in the standard co-flow laminar flame geometry employed that a near sooting flame is usually unattainable; with large dilution, most flames lift-off before soot formation can be eliminated. However, by simply interchanging the fuel and oxidizer streams and choosing the dilution of the streams appropriately, stable flames with no visible soot loading are readily attained. Measurements of temperature and intermediate hydrocarbon species for these so-called "inverse diffusion flames" (IDFs) of ethene, propene and 1-butene in near and slightly sooting conditions have been made. The effects of flame temperature and fuel structure on these profiles have also been measured.

The ready achievement of an inverse diffusion flame measurement makes a description of the experimental apparatus worthwhile in this part of the research. The geometry of the burner is similar to that of previous investigations (22) on "normal diffusion flames" (NDFs) and consists of a 1 cm diameter stainless steel central tube and an 8 cm outer shroud. The oxidizer is

a controllable mixture of  $O_2$  and  $N_2$  and flows through the central tube. The fuel flows in the outer stream and is heavily diluted with  $N_2$ . The inlet velocities of the two streams are always comparable.

The system is enclosed by a plexiglass chimney with mounted sampling probes and thermocouples fixed with respect to the chimney. The system is sealed to prevent ambient air contamination of the fuel. The entire chimney assembly is movable vertically and the probes are mounted on vernier scales so that profiles both axially (by moving the chimney) and radially are possible.

Gaseous samples were taken using an uncooled quartz micro-probe with an orifice of roughly 75 micrometers. The probe is vertical in the flame environment, roughly parallel to the streamlines. Samples are expanded from the flame to approximately 100 torr and subsequently compressed to 1 atmosphere for analysis using an HP-5840 Gas Chromatograph employing an FID. The GC/MS system was used to identify some unknown species. Some measurements of the permanent gases  $O_2$ ,  $N_2$ ,  $CO$  and  $CO_2$  were made with a Varian 920 GC employing a TCD.  $H_2$  concentrations were not measured.

Temperature measurements were made with a 6% Rh-Pt/30% Rh-Pt thermocouple with a 0.002 inch wire and coated with quartz to a diameter of 0.004 inches to prevent catalytic effects. No corrections for conduction or radiation were made.

The fuels tested were ethene, propene and 1-butene, all of C.P. grade. One ethene flame was sampled in detail and is considered as a base flame from which the effects of perturbations of the flame conditions can be observed. In all flames tested, the flame structure is kept similar by keeping the flame height and the parameter  $S = X_{O_2} / [X_f(n+m/4)]$  constant.  $X_{O_2}$  and  $X_f$  are the oxygen and fuel inlet mole fractions, and  $n$  and  $m$  are the carbon and hydrogen number of the fuel (24). For a given fuel, by changing the  $O_2$  and fuel concentrations together,

flames of similar structure but uniformly higher temperatures are obtained so that the effects of increased temperature on intermediate hydrocarbon concentrations at fixed residence times (25) are observed.

The initial measurements taken were chosen to isolate the effects of fuel structure and flame temperature on chemical fields which are near-sooting. Table 2 lists the flames sampled. The value  $S=1.5$  is held constant. The differences in flame height for a given fuel are due to differences in temperature which affects the diffusivity. The total central stream flow rate was kept constant for a given fuel at roughly 9 cc/sec. The total flow rates for different fuels were varied slightly owing to the different diffusivities between fuels and were made to match experimental flame height data. The outer stream flow rate was always 980 cc/sec. For flames in which soot was visible, it appeared outside the blue reaction zone. For faintly luminous flames there was no clogging of the sampling probe during the required sampling time. The hottest ethene flame did clog the probe in the regions where the soot loading was greatest and no data are available there.

The general character of the pyrolysis zone of any hydrocarbon IDF is demonstrated in Figure 8 which is a radial profile taken at the flame height for the base ethene flame. The unspecified species in this figure have not been identified with the GC/MS system but are primarily C4, C5 and C6 branched, unsaturated aliphatics. The intermediate hydrocarbons from pyrolysis reactions are most readily formed outside the flame front, where the temperature is high and no oxygen exists. They diffuse both into the flame where they are oxidized and away from the flame where their pyrolysis ceases due to the lower temperatures. When soot first becomes visible, it does so on the steep flame side of the intermediate peaks.

Profiles for the base flame at both lower and higher heights are surprisingly similar with regard to the peak concentrations of intermediates, and indicate a net balance between reaction and diffusion. Notable exceptions are for allene and di-acetylene; at a height of 5 mm, allene attains almost an order of magnitude higher concentration than it has at 19 mm (the flame ht) while di-acetylene is about three times lower at 5 mm than it is at 19 mm. At 12 mm height, the peak concentrations of all intermediates are close to what they are at 19 mm. For heights greater than the flame height, the intermediates begin to reach the centerline because there is no longer a flame to destroy them. Some of the species show slight increases in concentration due to post-flame reactions, but these are minor changes. In short, a radial profile at the flame height is indicative of the intermediate hydrocarbon field at any height; in particular, in the region where soot first appears.

The effect of flame temperature can be observed by comparing the concentrations of all intermediates for the five ethene flames tested which pass from nonsooting to sooting flames. A uniform increase in concentration of all intermediates is observed with increasing flame temperature (except propene which uniformly decreases). Di-acetylene has a much higher sensitivity than any other species. It is difficult to ascertain which species may participate in soot formation because any reduction in concentration due to particle formation is insignificant.

Fuel structure effects are demonstrated in Figures 9 and 10. The temperature profiles for all the flames at the flame height are reported in Figure 9. Flames 2, 6 and 8 are near-sooting flames. No attempt was made to match temperatures in choosing these three flames; rather, the criterion of near-sooting was imposed. The result is that the temperature profiles for the three

flames are quite close. The slightly sooting flame choice is much more ambiguous visually but again, the three temperature profiles are similar. The region where soot first appears is determined by the drift in thermocouple output in the slightly sooting flames.

That the temperature fields are quite similar for the near sooting flames is surprising at first glance in view of the different sooting tendencies of the fuels. However, a similar result for NDFs has been observed (26) in which the temperature at which soot first forms is the same (about 1300 K) for different fuels. In this study as well, the temperature is approximately 1300 K where soot formation begins in the slightly sooting flames. It appears that a critical temperature of approximately 1300 K must be exceeded in order to form particles in the resident times available in laminar diffusion flames, regardless of the fuel.

The temperature field similarity also allows more meaningful interpretation of concentration field comparisons. Figure 10 shows the effect of different fuels on the intermediate concentrations of near sooting flames. Radial plots at the flame height have been taken and the value of the peak concentration of each intermediate concentrations demonstrated in Figure 10 are:

- acetylene concentrations are high in all three flames, and are highest in the ethene flame.
- the butene and propene flames have about an order of magnitude higher concentration of propyne (and allene by partial equilibrium) than the ethene flame.
- di-acetylene and vinyl-acetylene are in comparable concentrations in all three flames. The butene flame has a higher concentration of butadiene.
- the concentrations of cyclo-pentadiene and the mono-aromatics benzene,

toluene, styrene, and phenyl-acetylene increase from ethene to propene to butene.

Interpretations of the possible mechanism of particle formation from the results of this study are not conclusive at this time, but are suggestive. Clearly, the requirements of sufficiently high temperature and sufficient high concentrations of hydrocarbon intermediates must be met. The identification of important species remains elusive. It appears, however, that the inception of particles may be insensitive to the concentrations of acetylene, methyl-acetylene, allene and mono-aromatics as these species vary widely in the three near sooting flames. That vinyl-acetylene and di-acetylene are found to have similar concentrations in all flames may indicate that they play a fundamental role in inception but may also be a coincidence. Future tests with different classes of fuels could clarify the roles of various intermediates in the inception of soot particles and is the current direction of this research.

#### C. High Energy Density (Boron) Slurry Vaporization/Combustion Processes

##### 1. Free Slurry Droplet Combustion

The experimental studies in burning of free slurry droplets have progressed substantially during the past year.

Despite the considerable attention that boron slurries have received in recent years as potential high energy density liquid fuels, very little fundamental work on the actual vaporization/combustion of isolated droplets have been reported to date. The primary purpose of the current study is to investigate the fundamental vaporization/combustion behavior of boron slurry droplets and to provide information useful for fuel and combustor development efforts. First observations on the combustion properties of isolated boron slurry droplets were reported in the previous contract period [27], particularly

focused on disruption phenomena of the primary slurry droplets. During the past year, the work was extended to boron/JP-10 slurries with various solid loadings including pure JP-10 fuel droplets. The results were presented at the Eastern States Section Meeting of the Combustion Institute [28] and the Twenty-First International Symposium on Combustion [29]. Currently, some preliminary experimental efforts are under way to collect condensed-phase combustion products to investigate both the role of condensation and the mechanism of disruption.

Observations of burning free droplets of both pure JP-10 and boron/JP-10 slurry fuels were made in a high-temperature, atmospheric-pressure, oxidizing environment under conditions of low Reynolds number. A stream of well-dispersed droplets (approximately 100 droplet diameters apart) was projected downward through the center of a premixed, water-cooled, flat-flame burner coaxially into a hot post-combustion gas stream. A droplet generation system utilizing an aerodynamic technique, which was developed in the previous contract period particularly for highly-viscous solid-containing liquid fuels, was used to produce small droplets (typically 350 - 450  $\mu$  diameter) of both pure JP-10 and boron/JP-10 slurry fuels. The flat-flame burner producing the post-combustion gases was operated at atmospheric pressure using fuel-lean mixtures of methane, oxygen, and nitrogen (Table 3).

Pure JP-10 fuel was tested to obtain basic information for interpreting the results on boron/JP-10 slurry fuels. The droplets ignited shortly after injection ( $<10$  ms) and an envelope diffusion flame developed. Figure 11(a) shows typical temporal variations in the droplet diameter ( $d$ ), the droplet velocity ( $U_d$ ), the gas velocity ( $U_g$ ), and the droplet Reynolds number ( $Re_d$ ) for two separate runs under the same condition of highest oxygen concentration (gas mix. no.: 1). The droplet of Run 1 had a smaller diameter than that of Run 2 and



therefore completed combustion sooner. Figure 11(b) shows the results for lower oxygen contents (gas mix. no.: 3 and 5) and exhibits slower vaporization, as expected. The termination of combustion was accompanied by a yellow flash extinction typical of hydrocarbon droplet combustion, except at the lowest oxygen content (gas mix. no.: 5), where no flash was seen.

Figure 12(a) shows the temporal variations in the square of the droplet diameter. The linearity supports the d-square law, i.e.;  $d^2 - d_0^2 = -Kt$ . The burning-rate constant ( $K$ ) determined from the slope of each line is shown in Fig. 12(b) as a function of the environmental oxygen mole fraction. As expected, the burning-rate constant increased as the oxygen content was increased. A theoretical curve obtained from the following equation is also plotted.

$$K = (8k/q_d c_p) \ln(1 + B), \quad (1)$$

$$B = \{c_p(T_g - T_b) + iY_{O_2}H\}/L. \quad (2)$$

Here,  $q_d$  = liquid density of JP-10 at  $T_b$  ( $0.806 \text{ g/cm}^3$ );  $T_b$  = boiling point of JP-10 ( $455\text{K}$ );  $c_p$  = specific heat of JP-10 at  $T = (T_b + T_f)/2$ ;  $T_f$  = adiabatic flame temperature of JP-10;  $B$  = transfer number;  $k = 0.4 k_{JP-10} + 0.6 k_{N_2}$  = thermal conductivity of the gas mixture at  $T = (T_b + T_f)/2$ ;  $i$  = stoichiometric fuel/oxidizer mass ratio ( $0.3$ );  $Y_{O_2}$  = environmental oxygen mass fraction;  $H$  = heat of combustion of JP-10 ( $10.1 \text{ kcal/g}$ );  $L$  = heat of vaporization of JP-10 ( $69.5 \text{ cal/g}$ ). The predicted burning-rate constant is in reasonably good agreement with the experimental values in spite of uncertainties in properties of gas mixtures. The stronger dependence on  $X_{O_2}$  in the experiment may be due to an increase in  $k/c_p$  from fuel pyrolysis with increasing  $X_{O_2}$ , not accounted for in the correlation approach.

Boron slurry droplets burned for short periods of time quiescently with an

envelope diffusion flame of vaporized JP-10, but then experienced pronounced disruption in all cases, except for the droplets of low solid loading ( $Y_B = 0.05, 0.1$ ) in the lowest oxygen environment (gas mix. no.: 5). Figure 13 shows the measured gas temperature ( $T_g$ ) and the adiabatic flame temperatures of JP-10 ( $T_{f,JP-10}$ ) along the centerline. The location at which the disruption occurs along each droplet trajectory is shown by cross-hatching for each of the gas mixtures and boron loadings. As the oxygen content was increased for a fixed boron mass fraction, the disruption occurred at earlier times. This is attributable to increased heat flux from the flame to the droplet surface as a result of both higher flame temperature and closer proximity of the flame to the surface. As the boron particle loading was decreased, the time to disruption increased significantly. At all solid loadings, if the diffusion flame temperature at the event of disruption is higher than the boiling point of  $B_2O_3$  (2316K), the greenish emission and popping sound, characteristic of boron ignition, were noticed. When boron ignition occurs, the boron particles ejected from the primary slurry droplet must ignite upon passing through the higher-temperature diffusion-flame zone and becoming exposed to the oxidizing environment. This exposure to oxygen leads to rapid onset of combustion without the intervening ignition stage of the type previously observed experimentally and analyzed theoretically.

Figure 14 shows temporal variations of the square of droplet diameter, with data on pure JP-10 ( $Y_B = 0$ ) also included. It is remarkable that the d-square plot for  $Y_B = 0.1$  shows a linear dependence in the initial period and that the slope of the decay line is the same as that of JP-10. This result indicates that the liquid component of the slurry with relatively low solid loading burns initially without any influence of the solids, thus concentrating the slurry

itself.

The process leading to disruption may be speculated as follows (see Fig. 15). It appears that the initial decay ends when the solid loading near the surface becomes sufficiently high to form a rigid shell of boron particles (see (c) in Fig. 15). While the shell is porous, as proposed in the rigid-porous-shell model by Antaki [30,31], vapor of JP-10 is able to pass through the shell. As the liquid surface regresses into the interior, the temperature of the shell surface may increase. When physical binding and/or dense agglomeration of boron particles occur at the surface, an impermeable shell appears to develop. Additives with high boiling points, which are expected to accumulate near the surface, may contribute to this process. Internal vaporization may then occur at heterogeneous nucleation sites just beneath the shell, further promoting pressure buildup that eventually results in disruption ((d) in Fig. 15).

Recently collected were quasi-spherical hollow shells of the boron agglomerate with blowholes, which lead experimental support to the hypothesis of the formation of the impermeable shell. Figure 6 shows a typical scanning electron micrograph of the shell collected at the exit of the combustion chimney. It is noticeable that the outer surface of the shell is smoother than the inner surface. The shell thickness is typically  $10 \pm 5 \mu$ . From the burning-rate data of JP-10, the shell thickness can be estimated by calculating the volume of JP-10 consumed in the period between the end of the initial diameter decay and the disruption event. The boron in the original slurry droplet was assumed to be left behind, immobile as the liquid vaporized. For both  $Y_b = 0.1$  and  $0.3$ , the resulting shell thickness was approximately  $20 \mu$ , which is somewhat thicker than the actual shell probably because of accumulation and compaction of particles in the layer during the liquid surface regression process.

As described above, some physical understanding leading to explanations of observed droplet-burning and disruption behavior was developed in the past year. It was established that although available theories are adequate for the approximate calculation of burning-rate constants in regimes in which the  $d^2$ -square law applies, estimations of conditions for departure from this law or of the character of the disruption processes cannot be obtained well from existing theories. Good bases for quantitative extrapolation of the results beyond the conditions of the present experiments therefore are unavailable. The physical ideas that have been proposed here should be used to develop quantitative theories for the termination of the  $d^2$ -square regime and for the disruption process. This is especially important because the disruptions observed here differ substantially in character from those found for other fuels such as liquid solutions or emulsions. If a successful quantitative theory is obtained for predicting the time to disruption and the associated mass loss found in the present experiments, then calculations for conditions in practical combustors can be made.

## 2. Boron Suspension (Cloud) Combustion

Experimental studies of ignition and combustion of boron particles have progressed through continuing research on boron suspension combustion. These studies are addressing concerns that under practical combustor conditions finite-rate chemical kinetics may lead to excessively long combustion times for boron particles. The objectives are to determine and understand burning rates of fine boron particles under conditions of chemical-kinetic control. The use of boron suspensions or clouds was adopted as a convenient way to approach studies of single-particle kinetics since for the particle sizes of interest (diameters  $< 5 \mu$ ) experiments with single particles would be prohibitively expensive. An

experimental apparatus was designed and constructed for measurements of combustion of boron suspensions, and various preliminary experimental results were obtained. In addition, theoretical studies progressed to relate the results of the experimental measurements to the behaviors of single boron particles.

An apparatus was constructed consisting of a flat-flame burner employing methane-oxygen-nitrogen mixtures. By adjusting flow rates of the reactants the flame temperature and oxygen concentration in the product gas can be varied independently. A particle feed system was designed and constructed for transporting particle suspensions in a nitrogen stream upward through a narrow tube in the center of the burner.

The performance of the feed system is a significant factor in the success of the experiment. In previous work a feed system had been obtained that operated successfully with  $\text{Al}_2\text{O}_3$  particles in the diameter range of 2 to 5  $\mu$ . The particle sizes of the acquired boron were in the range of about 0.2  $\mu$ , and the performance of the feed system was marginal with these smaller particles. The feed system therefore was modified to achieve desirable performance with smaller particles. In the current design the boron particles placed in a cylindrical chamber are agitated by a rotating blade driven by an electric motor, and the nitrogen carrier stream is split into two parts, one of which enters the chamber near the bottom and the other of which passes by the conically tapered top of the chamber. The independent controls are the total nitrogen flow rate, the bypass ratio and the speed of the electric motor. These controls can be adjusted to vary the boron particle loading at any fixed nitrogen flow rate.

The suspension fed through the central tube into the products of the flat-flame burner mixes and spreads as an axisymmetric laminar jet. The conservation equations for axisymmetric jet flow were employed as a basis for describing boron

particle histories in the experiment. For the region in which a similarity solution applies for the flow field the calculation of particle histories is easiest. Similarity profiles were obtained, and it was found that theoretically the optimum location for boron ignition in the jet occurs at the edge of the jet near the jet exit. Increasing residence times with increasing distance are offset by decreasing temperatures associated with mixing into the cold nitrogen from the jet and with heat loss from the burner products to the surroundings.

The experiments showed that three different types of boron flame configurations could be obtained upon injection of the boron suspension. At measured maximum temperatures of the flat flame below about 1700 K no luminosity from the boron suspension was observed. At temperatures between about 1700 K and 1800 K a dark yellow boron plume was visible with black smoke emitted from the top of it. At about 1800 K green emissions begin to appear around the edge of the yellow plume, but the green does not extend all the way to the centerline at the tip of the plume. As the temperature is increased further, the extent of the green increases, and at a third critical temperature it reaches the centerline, completely surrounding the yellow plume. Further increases in temperature result in a more intense green region surrounding a shortened but brighter yellow core.

Preliminary measurements were completed on the dependence of the critical temperatures identified above on the oxygen concentration in the product gas. Oxygen mole fractions were varied from about 0.1 to about 0.8, and it was found that over this range of conditions there was no significant influence of the oxygen content on the boundaries of the different types of flames. The occurrence of the different flame configurations depends mainly only on the flat-flame temperature. This observation is considered to support the possible significance of  $H_2O$  in boron ignition and oxidation.

For conditions under which the green luminosity extends to the centerline the height of the region of yellow luminosity may be a measure of the ignition times of the boron particles that travel along the centerline. This height was measured as a function of the flat-flame temperature for different jet velocities. It was found to increase with increasing jet velocity and to decrease with increasing flame temperature, as would be predicted from the expected corresponding variations in temperature-time histories of the particles. The strength of the dependence on flame temperature decreases with increasing flame temperature, and above about 2000 K there is no further discernible decrease in yellow height with increasing temperature. These yellow heights were found to be independent of the oxygen concentration in the product gas, within experimental accuracy. The implications of these observations on ignition processes are under continuing investigation.

To better evaluate the significance of the green emissions spectra of the green region of the flame were taken. In the experiment a He-Ne laser was used for alignment of lenses and a slit that focuses the green emissions onto the aperture of a polychrometer backed by a silicon-intensified detector. An optical multichannel analyzer served to convert the detector output into a spectrum displayed on an oscilloscope screen. The spectrum obtained matched quite well with the broad boric-acid fluctuation bands, attributed in the more recent literature to be associated with emissions from  $\text{BO}_2$ . These observations lend support to the hypothesis that the green emissions identify regions of chemical reactions of boron.

Spectra from the yellow regions are anticipated to be continua related to black-body emissions from hot boron particles. Spectral measurements are planned to be made to check this hypothesis. In addition, work is underway to obtain

samples from the flames by passing quartz microprobes through the flames and examining deposits by visible and scanning electron micrography. The sampling should help to clarify questions concerning the extent of combustion of boron in these experiments.

In general it may be stated that the research on boron suspension combustion is progressing somewhat more quickly than originally envisioned and that useful information concerning ignition and combustion times and their interpretations may emerge during the next year.



## REFERENCES

- 1) Brezinsky, K., Litzinger, T.A. and Glassman, I.; *Int.J. Chem. Kinet.* 16, 1053 (1984).
- 2) Litzinger, T.A., Brezinsky, K. and Glassman, I.; *Combust. Flame*, 63, 251 (1986).
- 3) Litzinger, T.A., Brezinsky, K. and Glassman, I.; *Combust. Sci. Tech.*, accepted for publication, 1986.
- 4) Venkat, C., Brezinsky, K. and Glassman, I.; *I. Symp.(Int.) Combust*; 19, 143 (1983).
- 5) Brezinsky, K.; *Prog. Energy Combust. Sci.* 12, 1 (1986).
- 6) Westbrook, C.K., Creighton, J., Lund, C., and Dryer, F.L.; *J. Phys. Chem.* 81, 2542 (1977).
- 7) Westbrook, C.K. and Dryer, F.L.; *Prog. Energy Combust. Sci.* 10,1 (1984).
- 8) Westbrook, C.K. and Pitz, W.J.; *Comb. Sci. and Tech.* 37, 117 (1984).
- 9) Pitz, W.J., Westbrook, C.K., Proscia, W.M. and Dryer, F.L.; *I. Symp.(Int.) Combust.* 20, 831 (1984).
- 10) Litzinger, T.A., Brezinsky, K. and Glassman, I.; *J.Phys.Chem.* 90, 508 (1986).
- 11) Litzinger, T.A., Ph.D. Thesis, Dept. Mech. and Aero. Eng., Princeton Univ., 1986.
- 12) McMillen, D.F. and Golden, D.M.; *Ann. Rev. Phys. Chem.* 33, 493 (1982).
- 13) Wilt, J.W.; "Free Radical Rearrangements", Free Radicals (J.K. Kochi, Ed.), John Wiley and Sons, N.Y. 1973.
- 14) Smith, R.D.; *J.Phys.Chem.* 83, 1553 (1979).
- 15) Robaugh, D.A. and Stein, S.E.; *Int.J.Chem.Kinet.* 13, 445 (1981).
- 16) Robaugh, D.A., Barton, B.D. and Stein, S.E.; *J.Phys.Chem.* 85, 2378 (1981).
- 17) Tsang, W.; "Comparative-Rate Single Pulse Shock Tube Studies on the Thermal Stability of Polyatomic Molecules", Shock Waves in Chemistry (A. Lifshitz, Ed.), Dekker, N.Y. 1981.
- 18) Yetter, R.A., Dryer, F.L. and Rabitz, H. ; *I. Symp.(Int.) Combust.* 21, (1986), accepted.
- 19) Larson, C.W., Chua, P.T. and Rabinovitch, B.S.; *J.Phys.Chem.* 76, 2507 (1972).

- 20) Glassman, I., AFOSR Tech. Rep. No. 79-1147 (1979).
- 21) Takahashi, F. and Glassman, I.; Comb. Sci. and Tech. 37, 1 (1984).
- 22) Gomez, A., Sidebotham, G., and Glassman, I.; Combustion and Flame 58, 45 (1984).
- 23) Glassman, I., "Combustion, 2nd Ed.", Academic Press, San Diego, CA, 1986.
- 24) Roper, F.G., Smith, C. and Cunningham, A.C.; Combustion and Flame 29, 227 (1977).
- 25) Santoro, R.J., Semerjian, H.G., and Dobbins, R.A., Combustion and Flame 29, 227 (1977).
- 26) Gomez, A. and Glassman, I.; 21st Symp. (Int.) Combustion; accepted for publication.
- 27) Takahashi, F., Dryer, F.L., and Williams, F.A., AFOSR TR-85-0559, May 1985.
- 28) Takahashi, F., Dryer, F.L., and Williams, F.A., Eastern States Section: The Combustion Institute Meeting, Paper No. 19, November 1985.
- 29) Takahashi, F., Dryer, F.L., and Williams, F.A., Twenty-First Symposium (International) on Combustion, The Combustion Institute, Pittsburgh, Pennsylvania, 1986 (in press).
- 30) Antaki, P.: Combustion Sci. Tech. 46, 113 (1985).
- 31) Antaki, P.: Department of Mech. and Aero. Eng., Princeton University, Ph.D. Thesis, 1985.

Table 1

N-Butyl Benzene Oxidation Mechanism and the Analogous Reaction for the Oxidation of n-Butane. ( $X \equiv OH, O, H$ ;  $\phi \equiv C_6H_5$ )

Abstraction

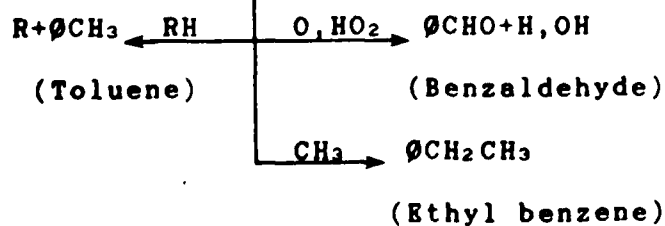
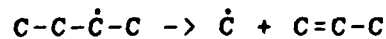
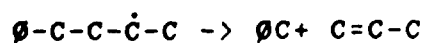
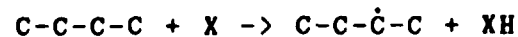
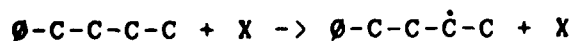
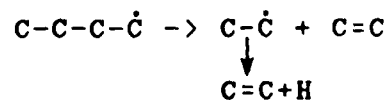
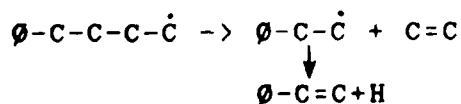
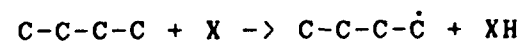
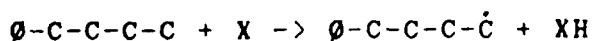
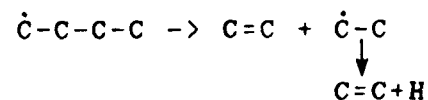
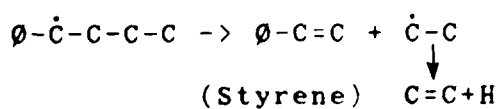
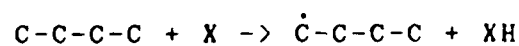
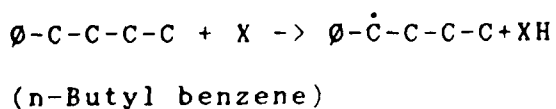
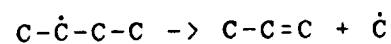
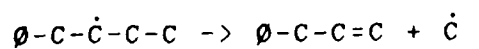
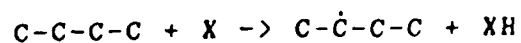
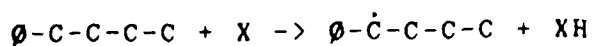


Table 1 continued



(Propenyl benzene)

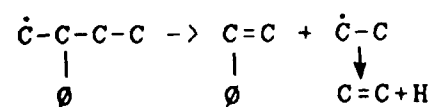
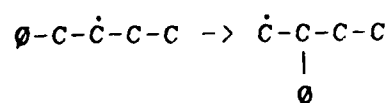
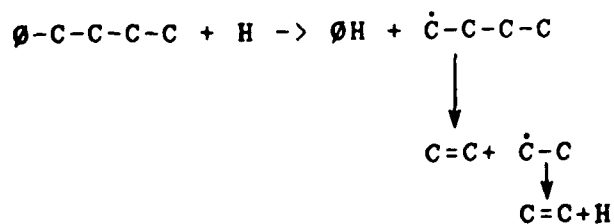
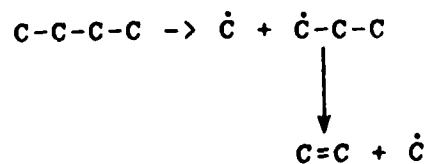
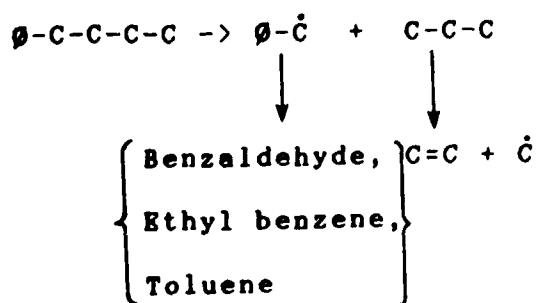
DisplacementHomolysis

TABLE 2

fuel	Xf	Xo2	flame ht(mm)	Peak axial temperature	Sooting condition
1) ethene	0.07	0.31	20.8	1550K	non-sooting
2) ethene (base)	0.083	0.36	19.4	1677K	near-sooting
3) ethene	0.09	0.39	18.3	1759K	slightly sooting
4) ethene	0.10	0.44	17.5	1860K	sooting
5) ethene	0.12	0.53	16.6	-----	sooting
6) propene	0.05	0.36	21.2	1642K	near-sooting
7) propene	0.06	0.41	19.2	1733K	slightly sooting
8) 1-butene	0.043	0.39	21.4	1588K	near-sooting
9) 1-butene	0.05	0.45	20.3	1745K	slightly sooting

TABLE 3 Burner Operating Conditions and Estimated Gas Mixture Compositions

Gas mix. no.		Flow Rate (l/min)			$T_{f, CH_4}$ (K)	Mole Fraction			
		CH <sub>4</sub>	O <sub>2</sub>	N <sub>2</sub>		X <sub>O2</sub>	X <sub>N2</sub>	X <sub>CO2</sub>	X <sub>H2O</sub>
1	0.3	10.0	66.7	43.3	2054	0.39	0.36	0.08	0.17
2	0.4	10.0	50.0	60.0	2065	0.25	0.50	0.08	0.17
3	0.5	10.0	40.0	70.0	2073	0.17	0.58	0.08	0.17
4	0.6	10.0	33.3	76.7	2078	0.11	0.64	0.08	0.17
5	0.7	10.0	28.6	81.4	2086	0.07	0.68	0.08	0.17

## FIGURE CAPTIONS

- FIGURE 1 Selected species profiles from the slightly lean ( $\Phi=0.98$ ) oxidation of n-butyl benzene.  $C_{10}H_{14}$ : n-butyl benzene,  $C_2H_4$ : ethylene,  $C_8H_{10}$ : ethyl benzene,  $C_8H_8$ : styrene,  $C_8H_6$ : phenyl acetylene.
- FIGURE 2 Selected species profiles.  $C_7H_6O$ : benzaldehyde,  $C_7H_8$ : toluene,  $C_6H_6$ : benzene,  $C_6H_5O$ : phenol,  $C_9H_{10}$ : propenyl benzene.
- FIGURE 3 Selected species profiles.  $C_{14}H_{14}$ : dibenzyl,  $C_3H_6$ : propylene,  $CH_4$ : methane,  $C_2H_6$ : ethane,  $C_2H_2$ : acetylene.
- FIGURE 4 Temperature, total carbon, oxygen and carbon monoxide profiles from the slightly lean oxidation of n-butyl benzene.
- FIGURE 5 Plot of the fuel profile against reaction time demonstrating the exponential decay over two orders of magnitude.
- FIGURE 6 Simple, general reaction mechanism for the oxidation of n-alkyl benzenes.
- FIGURE 7 Major species profiles from the oxidation of m-xylene.
- FIGURE 8 Base ethene flame; radial profiles at flame height. Key to Fig. 8; 1 - ethene, 2 -  $CO_2$ , 3 -  $CO$ , 4 -  $C_2H_2$ , 5 -  $CH_4$ , 6 - 1,3 butadiene, 7 - vinyl-acetylene, 8 - di-acetylene, 9 -  $C_2H_6$  (fuel contam.), 10 -  $C_3H_6$ , 11 - propyne, 12 - benzene, 13 - allene, 14 - cyclopentadiene, 15 - toluene, 16 - phenyl-acetylene, 17 - styrene.
- FIGURE 9 Temperature profiles at flame height
- |           |           |
|-----------|-----------|
| ○ Flame 4 | ◇ Flame 2 |
| ◆ Flame 3 | □ Flame 6 |
| ▼ Flame 9 | ▽ Flame 8 |
| ■ Flame 7 | ● Flame 1 |
- FIGURE 10 Peak concentrations of intermediates for near sooting flames. Same key as Fig. 9.
- FIGURE 11 Temporal variations of droplet diameter, droplet velocity, gas velocity, and Reynolds number of JP-10 droplets.  $\diamond$   $\blacklozenge$ , d;  $\square$   $\blacksquare$ ,  $U_d$ ;  $\triangle$   $\blacktriangle$ ,  $U_g$ ;  $\nabla$   $\blacktriangledown$ ,  $Re_d$ . (a) Gas mix. no. 1. Open, run 1; filled, run 2. (b) Gas mix. no.: open, 3; filled, 5.
- FIGURE 12 (a) Temporal variations of d-square of JP-10 droplets. Gas mix. no.:  $\diamond$ , 1 (run 1,  $d_o = 0.36$  mm);  $\square$ , 1 (run 2,  $d_o = 0.39$  mm);  $\triangle$ , 3 ( $d_o = 0.39$  mm);  $\nabla$ , 5 ( $d_o = 0.35$  mm). (b) Burning-rate constant of JP-10 droplets as a function of environmental oxygen mole fraction.

- FIGURE 13 Variations of the adiabatic flame temperatures of JP-10 and the measured gas temperatures along droplet trajectories. Gas mix. no.:  $\diamond$ , 1;  $\square$ , 3;  $\nabla$ , 5.
- FIGURE 14 Temporal variations of d-square of boron/JP-10 slurry droplets. Gas mix. no.: 1.  $Y_B$ :  $\diamond$ , 0 (JP-10,  $d_o = 0.36, 0.39$  mm);  $\nabla$ , 0.1 ( $d_o = 0.53$  mm);  $\triangle$ , 0.3 ( $d_o = 0.44$  mm).
- FIGURE 15 Schematic illustration of the disruption mechanism.
- FIGURE 16 Scanning electron micrograph of the boron agglomerate shell (100X). Gas mix. no.: 1,  $Y_B = 0.3$ .



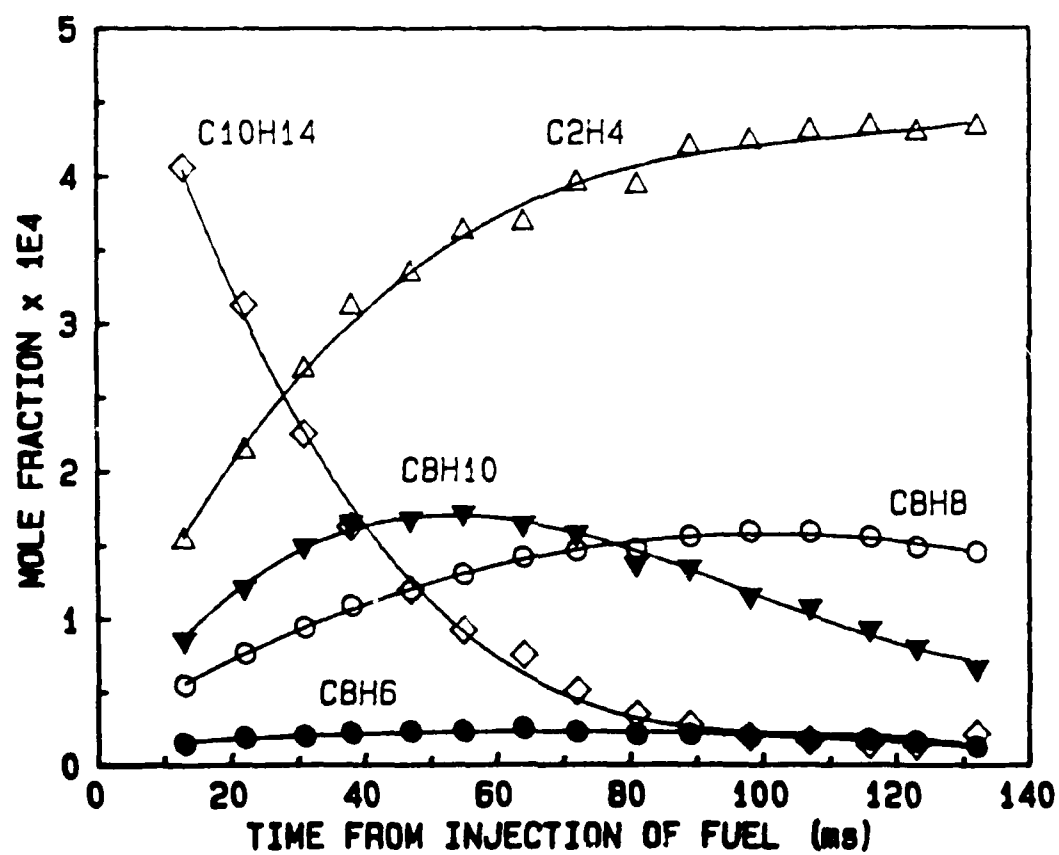


FIG. 1

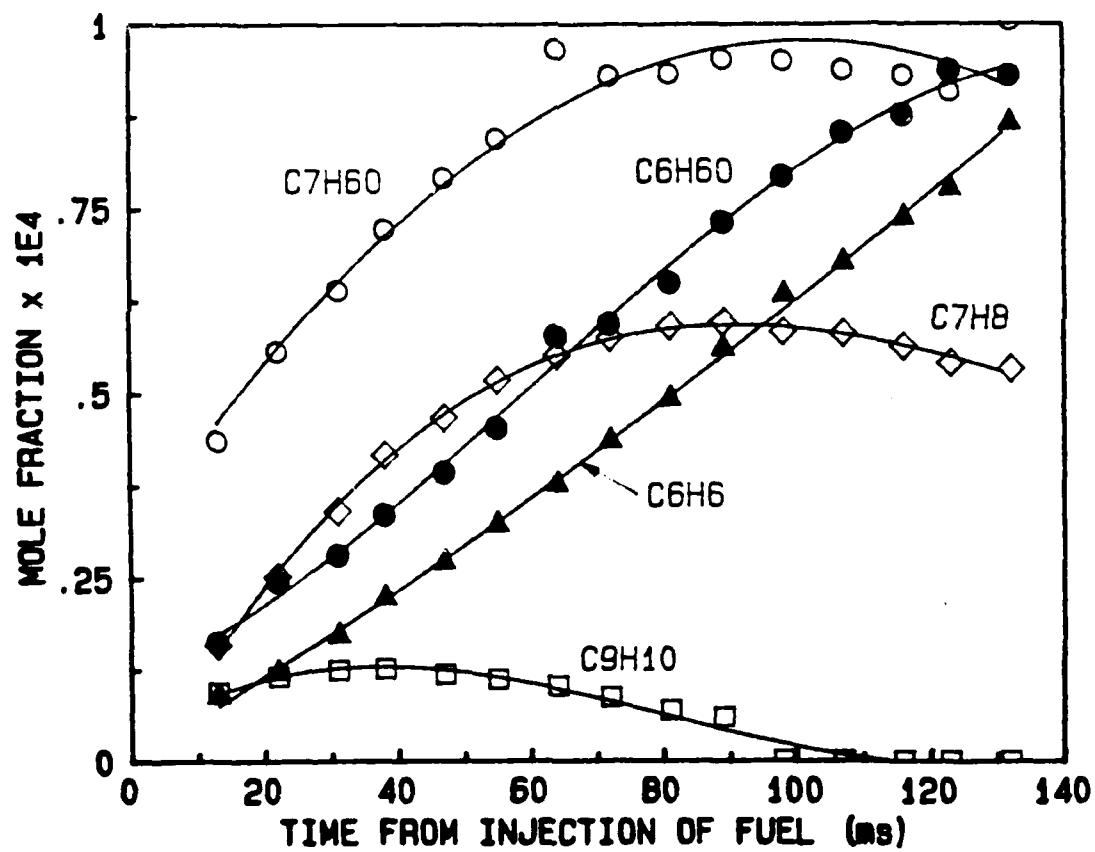


FIG. 2

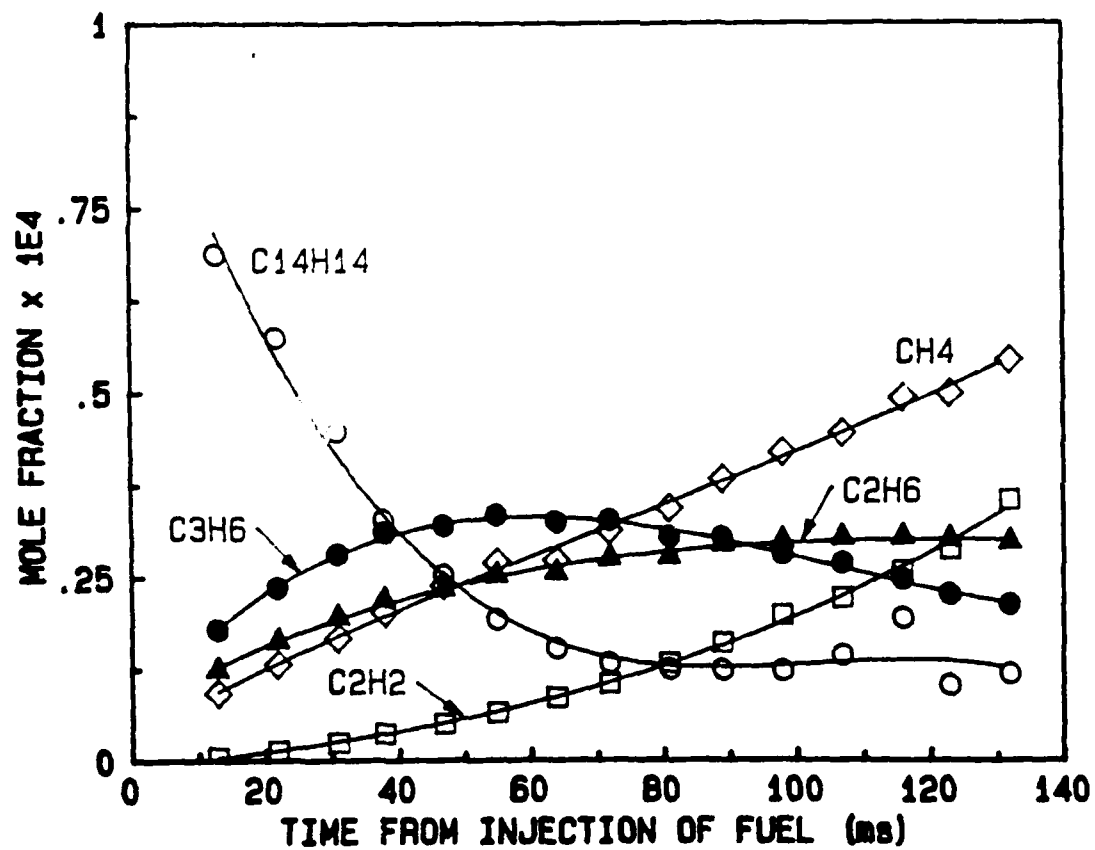


FIG. 3

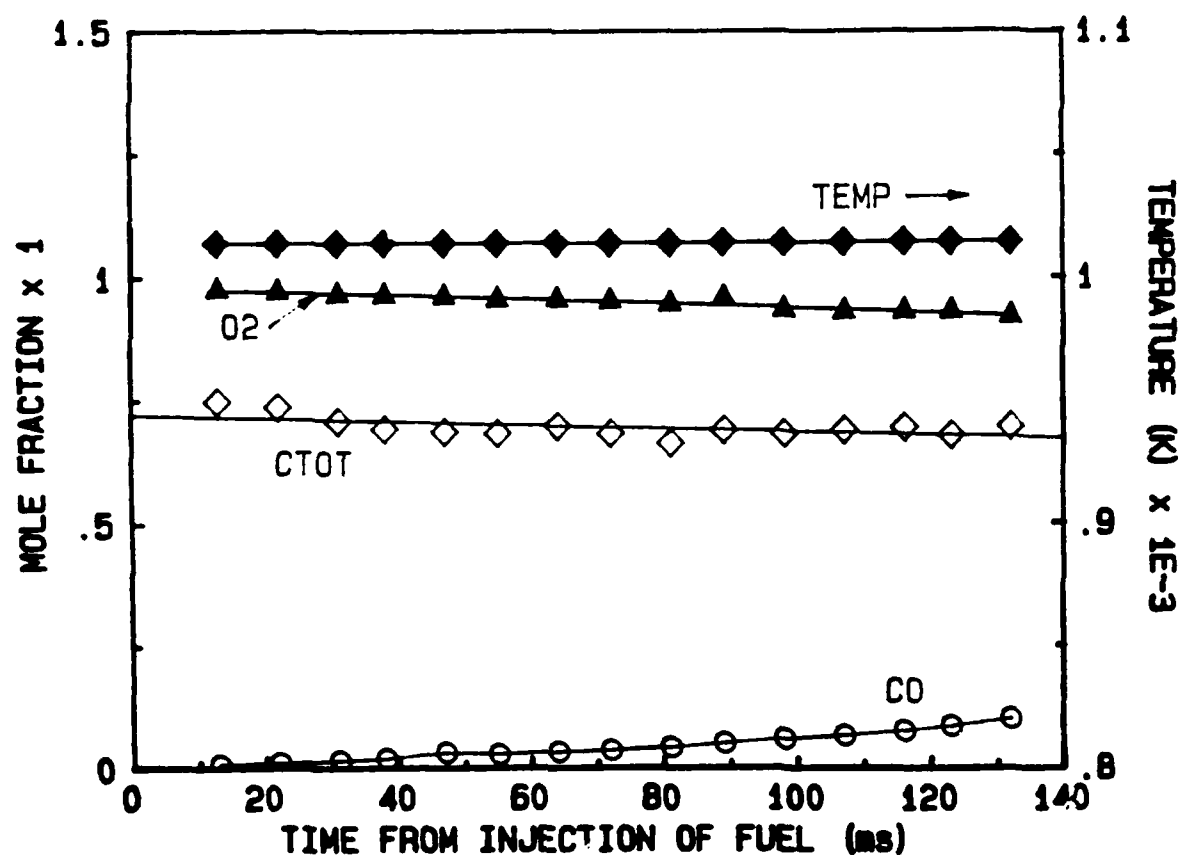


FIG. 4

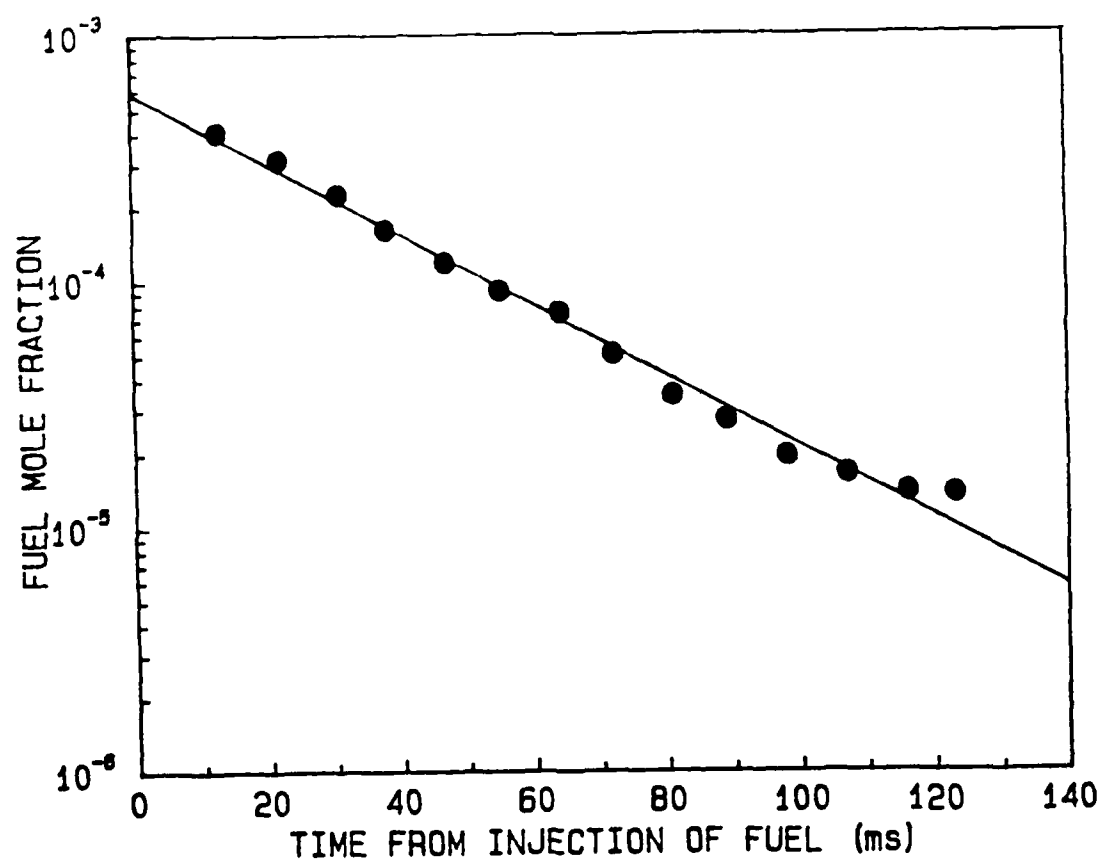


FIG. 5

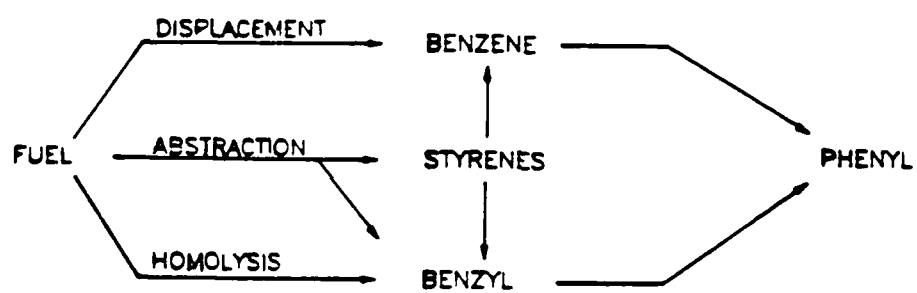


FIG. 6

# *m*-Xylene Oxidation

$\Phi = 1.03$   $T_0 = 1190$  K

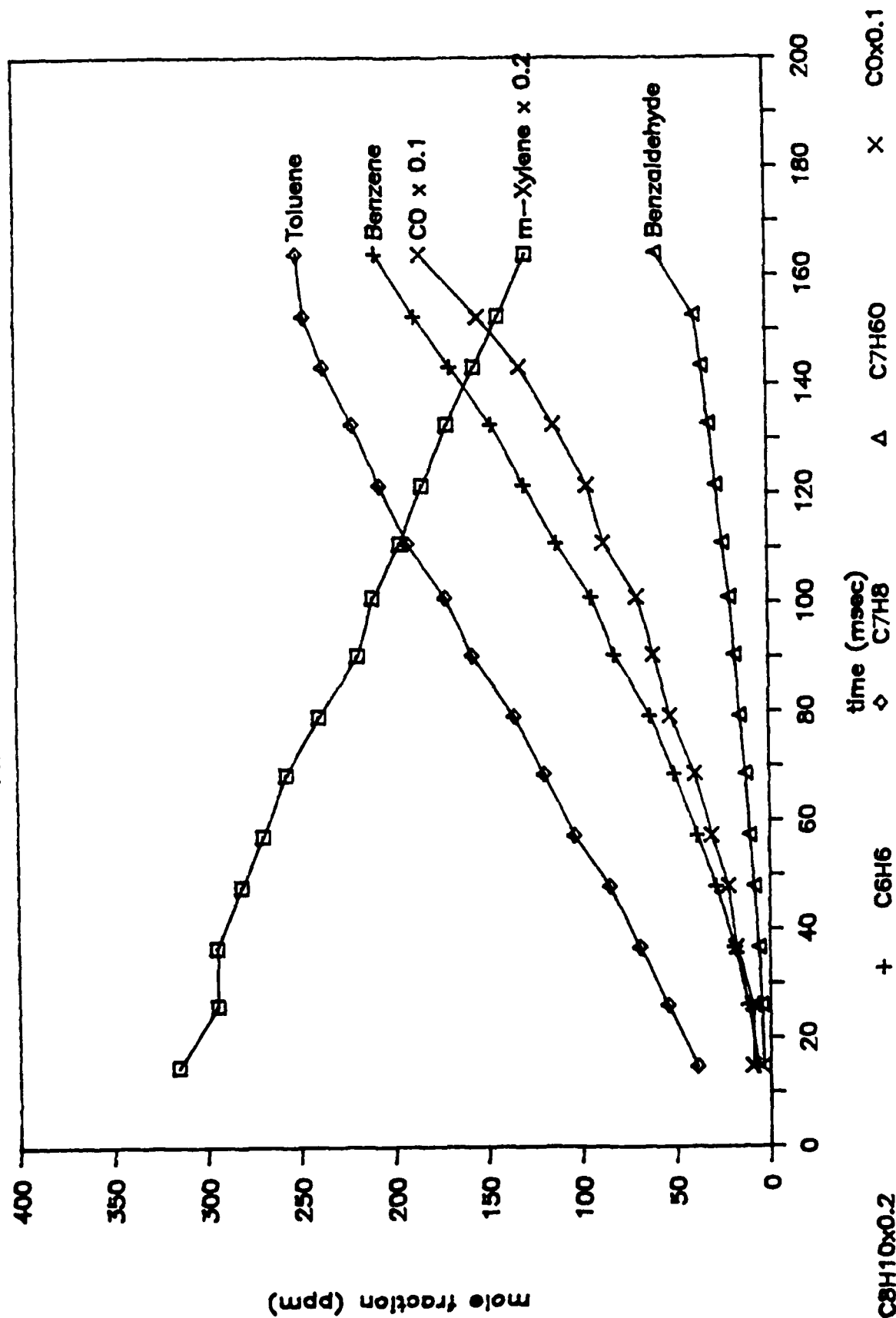


FIG. 7

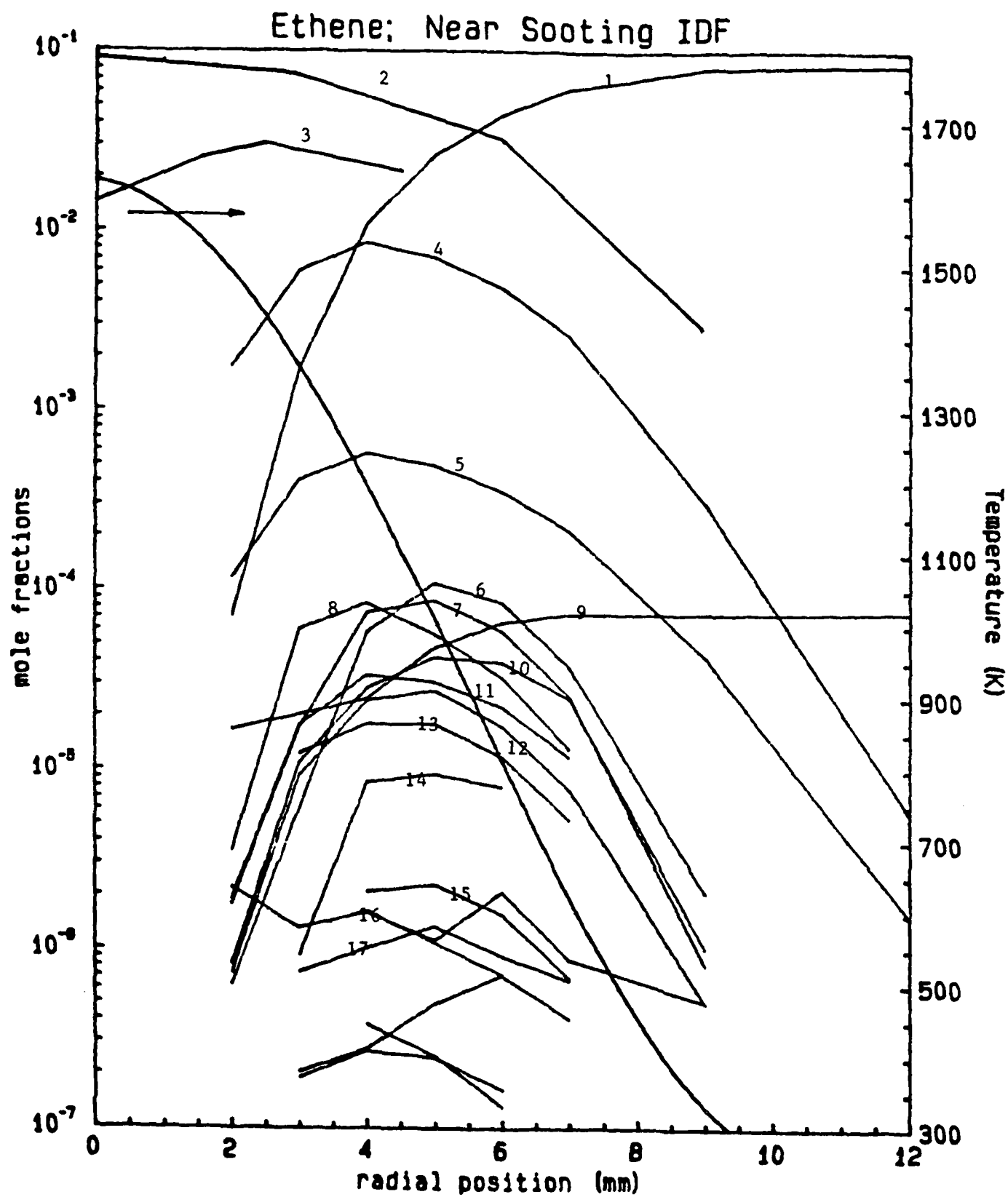


FIG. 8



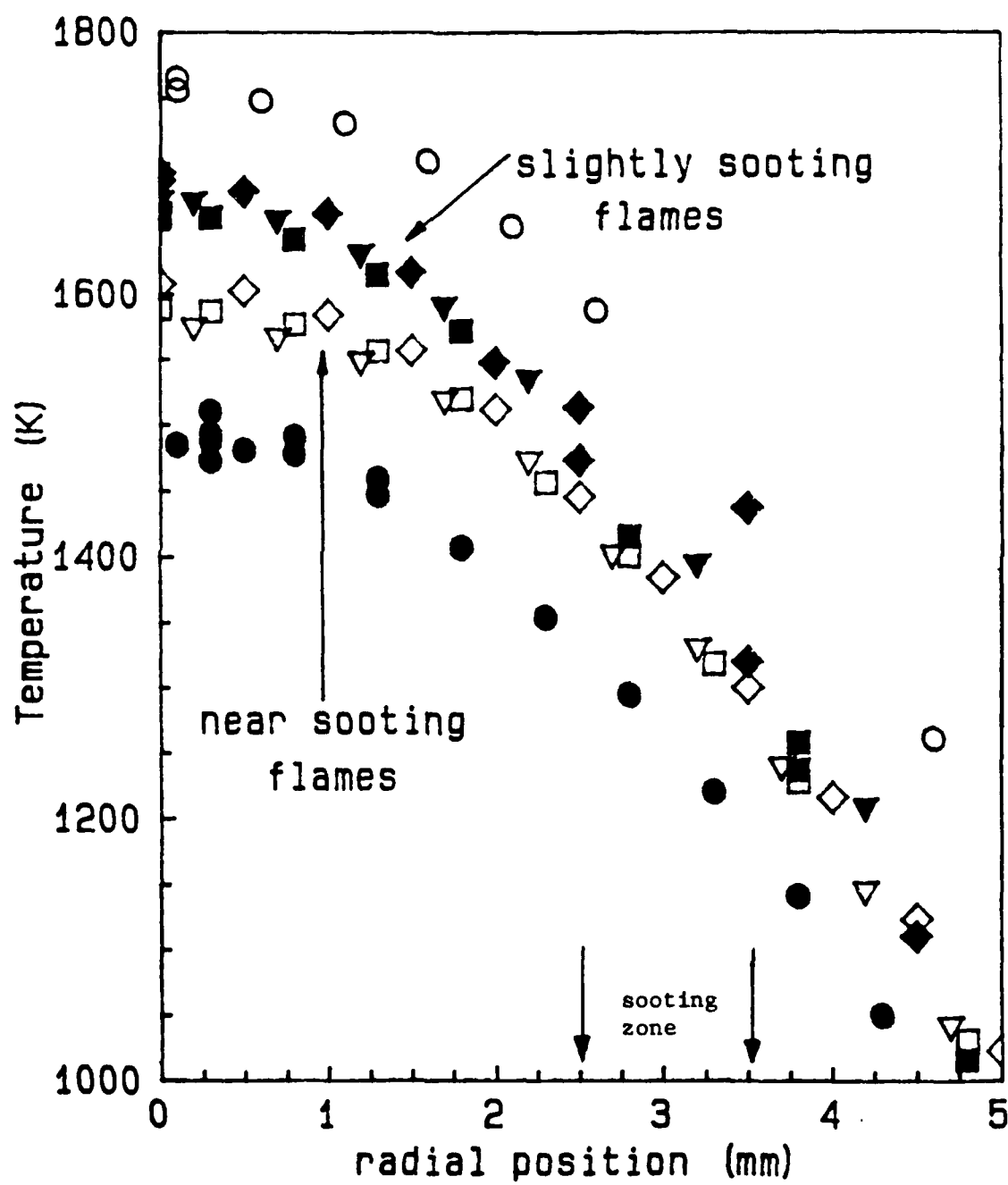


FIG. 9

# Near-Sooting IDFs

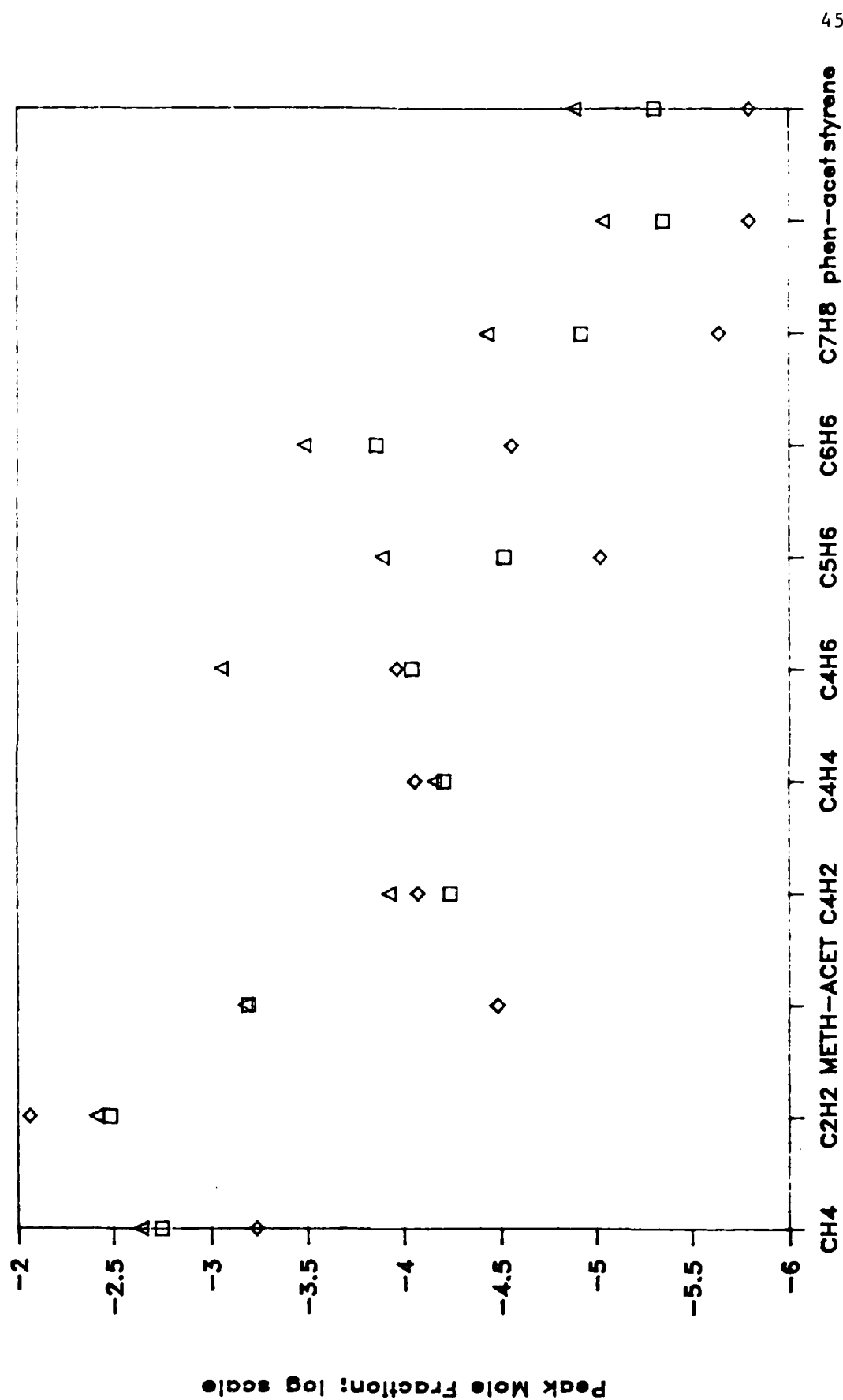


FIG. 10

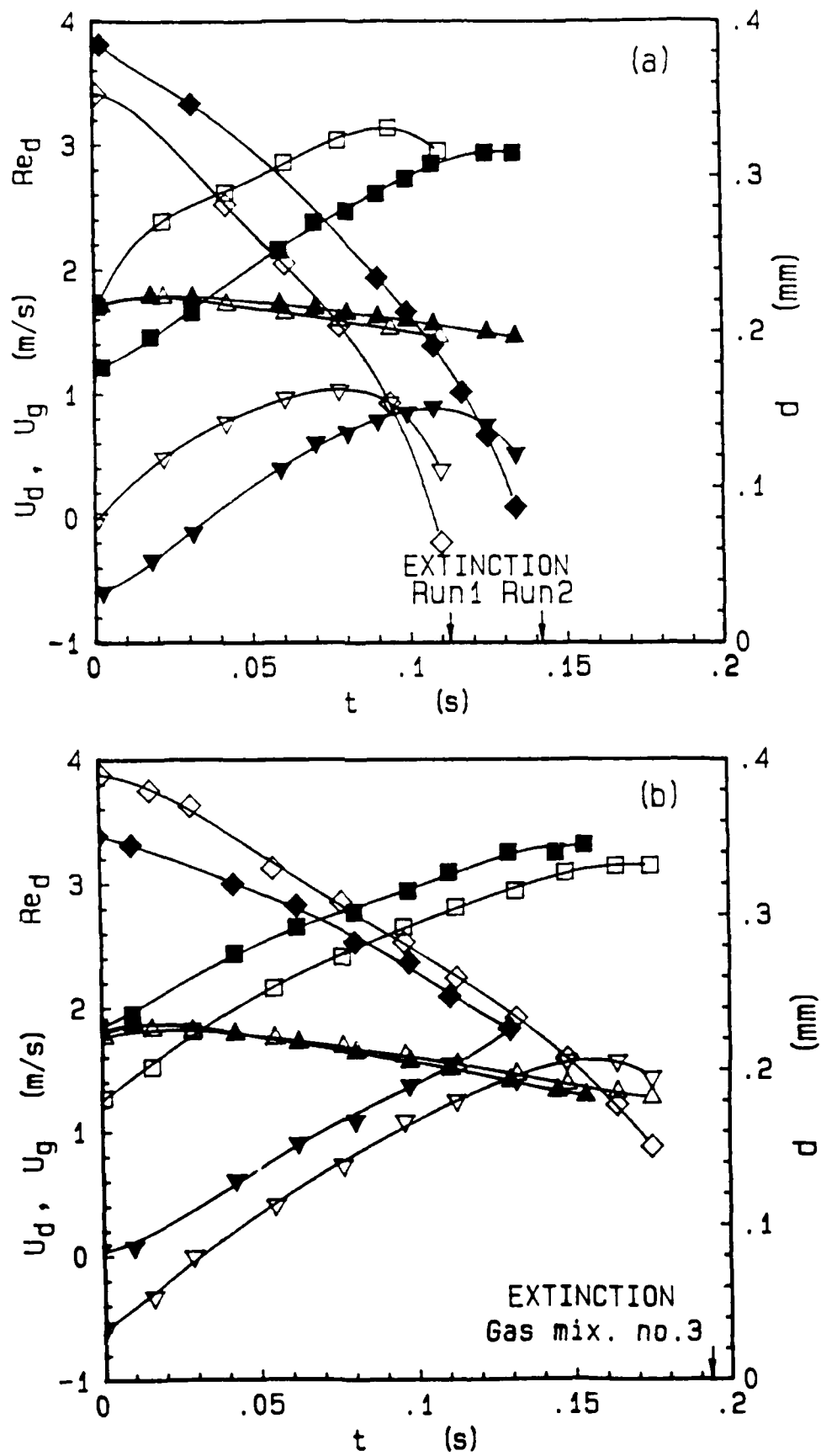


FIG. 11

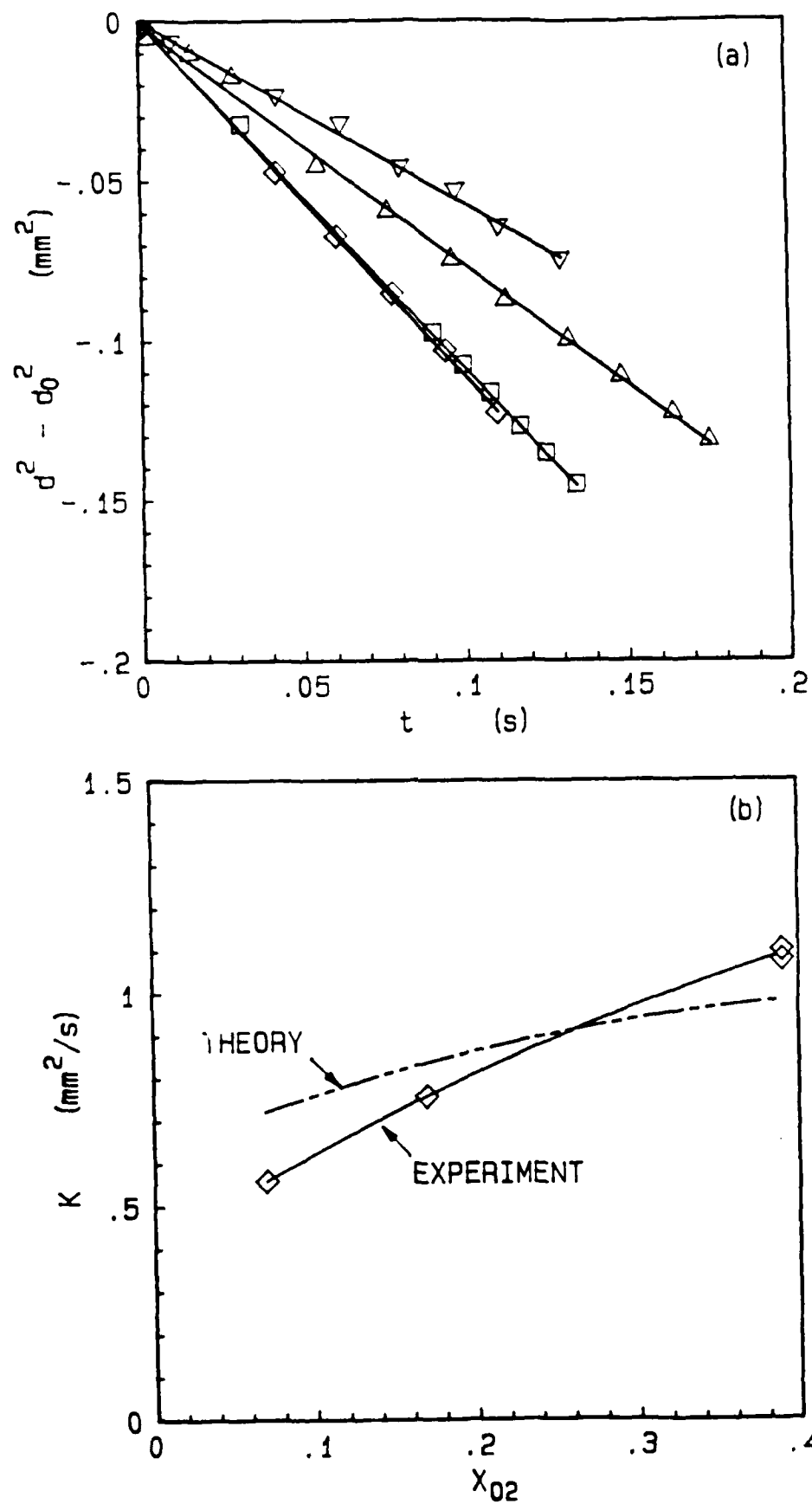


FIG. 12



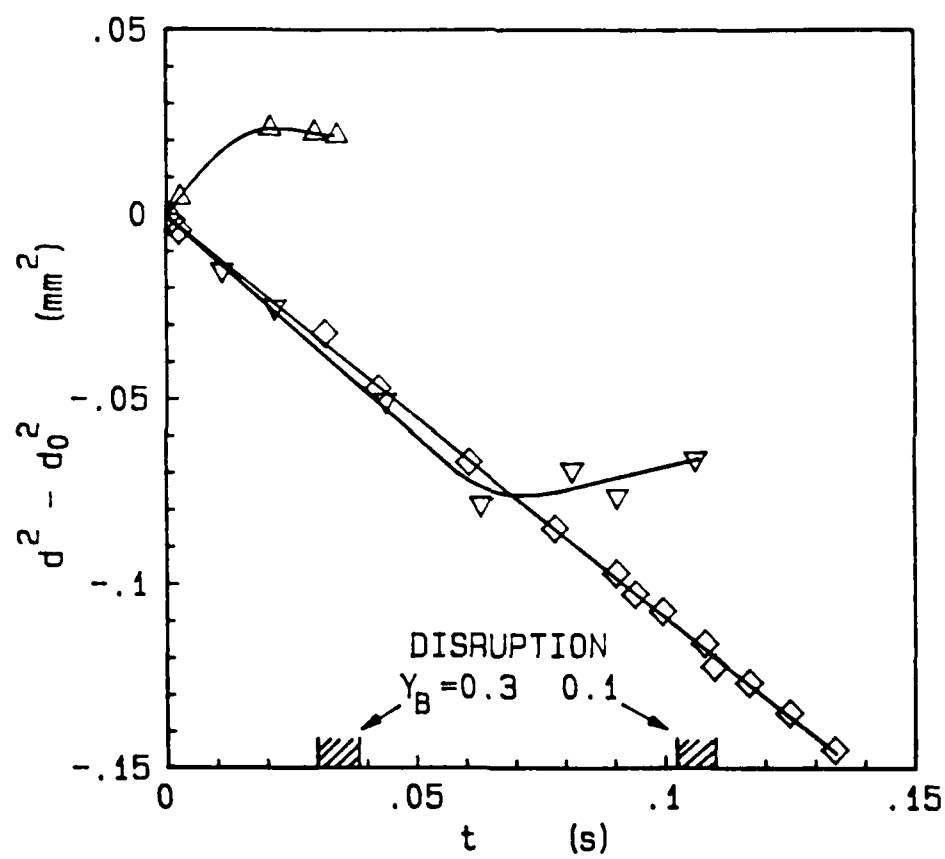


FIG. 14

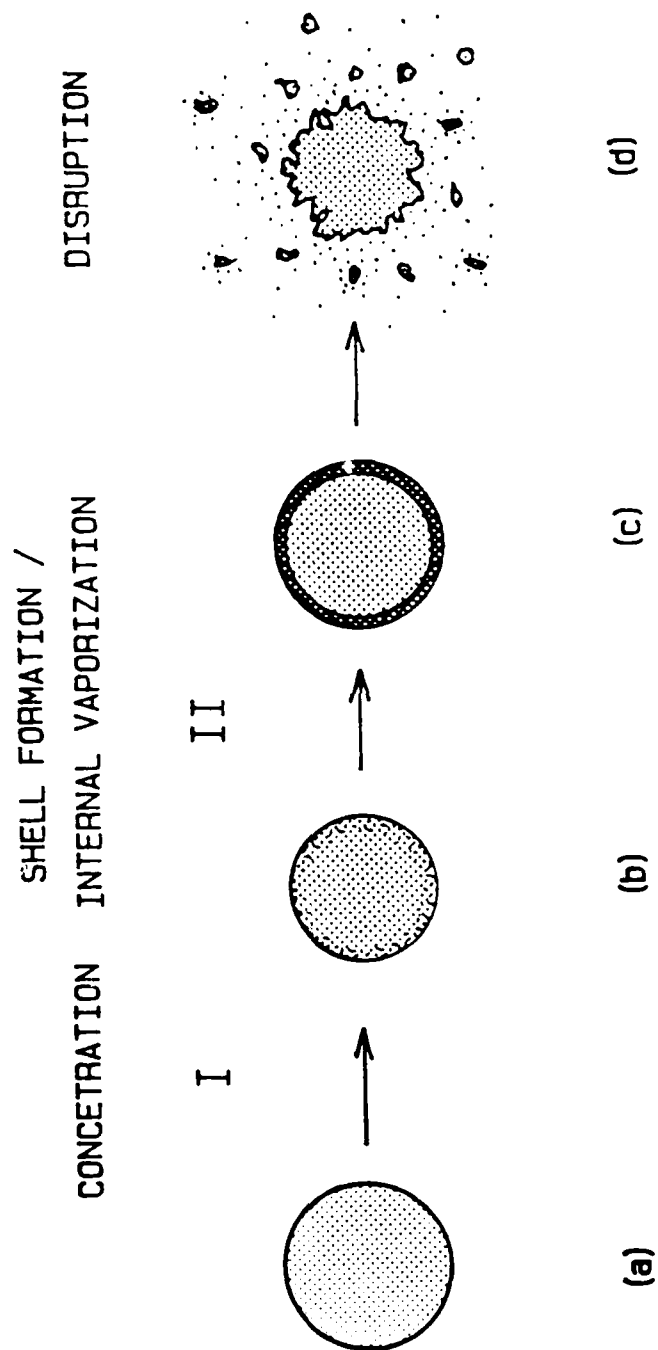


FIG. 15



FIG. 16



## III. Publications Related to Current Effort

1. F.L. Dryer and I. Glassman, "Combustion Chemistry of Chain Hydrocarbons," in "Alternative Hydrocarbon Fuels: Combustion and Chemical Kinetics," AIAA Series of Progress in Astronautics and Aeronautics, Vol. 62, p. 255 (1978), AIAA, New York.
2. R.J. Santoro and I. Glassman, "A Review of Oxidation of Aromatic Compounds," Combustion Science and Technology 19, 161 (1979).
3. D.J. Hautman, F.L. Dryer, K.P. Schug and I. Glassman, "A Multiple-Step Overall Kinetic Mechanism for the Oxidation of Hydrocarbons," Combustion Science and Technology 25, 219 (1981).
4. C. Venkat, K. Brezinsky, and I. Glassman, "High Temperature Oxidation of Aromatic Hydrocarbons," 19th Symp. (Int'l.) on Combustion, The Combustion Institute, Pittsburgh, p. 143, (1982).
5. K. Brezinsky, T.A. Litzinger, and I. Glassman, "The High Temperature Oxidation of the Methyl Side Chain of Toluene," Int. J. Chem. Kinetics 16, 1053 (1984).
6. T.A. Litzinger, K. Brezinsky, and I. Glassman, "Some Further Results on the Toluene Oxidation Mechanism," Eastern States Section: The Combustion Institute Meeting, Paper No. 69, December 1982.
7. T.A. Litzinger, K. Brezinsky, and I. Glassman, "Some Further Results on the Oxidation of Ethyl Benzene," Eastern States Section: The Combustion Institute Meeting, Paper No. 3, November 1983.
8. T.A. Litzinger, K. Brezinsky, and I. Glassman, "A Comparison of Results from the Oxidation of Normal and Isopropyl Benzene," Eastern States Section: The Combustion Institute Meeting, Paper No. 90, November 1984.
9. T.A. Litzinger, K. Brezinsky and I. Glassman, "The Role of Selectivity for Radical Abstraction of Hydrogen Atoms in the Oxidation of Normal and Isopropyl Benzene", to be presented at the International Conference on Chemical Kinetics, National Bureau of Standards, June 1985.
10. A. Gomez, G. Sidebotham and I. Glassman, "Sooting Behavior in Temperature Controlled Laminar Diffusion Flames," Comb. and Flame 58, 45 (1984).
11. K. Brezinsky, E.J. Burke and I. Glassman, "The High Temperature Oxidation of Butadiene," 20th Int'l. Symposium on Combustion, p. 613 (1984).
12. I. Glassman, "Phenomenological Models of Soot Processes in Combustion Systems," AFOSR Technical Report No. 79-1147 (1979).

13. K.P. Schug, Y. Manheimer-Timnat, P. Yaccarino and I. Glassman, "Sooting Behavior of Gaseous Hydrocarbon Diffusion Flames and the Influence of Hydrocarbons," *Combustion Science and Technology* 22, 235 (1980).
14. I. Glassman and P. Yaccarino, "The Effect of Oxygen Concentration on Sooting Diffusion Flames," *Combustion Science and Technology* 24, 107 (1980).
15. I. Glassman and P. Yaccarino, "The Temperature Effect in Sooting Diffusion Flames," 18th Int'l. Symposium on Combustion, The Combustion Institute, Pittsburgh, PA (1981).
16. Lt. K.E. van Teuren, "Sooting Characteristics of Liquid Pool Diffusion Flames," M.S.E. Thesis, Department of Mechanical and Aerospace Engineering, Princeton University (1978).
17. G. Sidebotham and I. Glassman, "Sooting Behavior of Cyclic Hydrocarbons in Laminar Diffusion Flames," Eastern States Section, The Combustion Institute Meeting, Paper No. 61, November 1983.
18. K.P. Schug, Y. Manheimer-Timnat, P. Yaccarino and I. Glassman, "Sooting Behavior of Gaseous Hydrocarbon Diffusion Flame and the Influence of Hydrocarbons," *Combustion Science and Technology* 22, 235 (1980).
19. I. Glassman and P. Yaccarino, "The Temperature Effect in Sooting Diffusion Flames," 18th Int'l. Symposium on Combustion, The Combustion Institute, Pittsburgh, PA (1981).
20. G. Sidebotham and I. Glassman, "Soot Formation in Laminar Diffusion Flames of Benzene II-Hexene Mixtures," Eastern States Section: The Combustion Institute Meeting, Paper No. 97, December 1985.
21. F. Takahashi and I. Glassman, "Sooting Correlations for Premixed Flames," Eastern States Section: The Combustion Institute Meeting, Paper No. 56, December 1982.
22. F. Takahashi and I. Glassman, "Interpretation of Sooting Correlations Under Premixed Conditions," Eastern States Section: The Combustion Institute Meeting, Paper No. 12, November 1983.
23. F. Takahashi and I. Glassman, "Sooting Correlations for Premixed Flames," *Combustion Science and Technology* 37, 1 (1984).
24. F. Takahashi, J. Bonini, and I. Glassman, "Further Experiments and Analysis of the Sooting Tendency of Premixed Fuels," Eastern States Section: The Combustion Institute Meeting, Paper No. 98, December 1985.
25. I. Glassman, F.A. Williams and P. Antaki, "A Physical and Chemical Interpretation of Boron Particle Combustion," 20th Int'l. Combustion Symposium, p. 2057 (1984).

26. P. Antaki, "Transient Processes in Slurry Droplets During Liquid Vaporization and Combustion," Eastern States Section, The Combustion Institute Meeting, Paper No. 62, December 1984.
27. P. Antaki, "Transient Processes in a Rigid Slurry Droplet During Liquid Vaporization and Combustion," Combustion Science and Technology, 46, 113 (1986).
28. F. Takahashi, F.L. Dryer and F.A. Williams, "Combustion Behavior of Free Boron Slurry Droplets," Central and Western States Section, The Combustion Institute Meeting, Paper No. 2-2B, April 1985.
29. Y.T. Loo, I.M. Kennedy and F.L. Dryer, "Disruptive and Micro-explosive Combustion of Free Droplets in Highly Connective Environments," Combust. Sci. and Tech. 41, 291 (1984).
30. P. Antaki, "Transient Processes in a Non-Rigid Slurry Droplet During Liquid Vaporization and Combustion," Combust. Sci. and Tech. 49, 289 (1986).
31. A. Gomez, M. Littman and I. Glassman, "Comparative Study of the Sooting Behavior of an Aromatic Versus an Aliphatic in Diffusion Flames," Western States Section/The Combustion Institute, Paper No. 6-7A (1986).
32. T.A. Litzinger, K. Brezinsky and I. Glassman, "Reaction of n-Propyl Benzene During Gas Phase Oxidation," Comb. Sci. and Tech. 50, 117 (1984).
33. T.A. Litzinger, K. Brezinsky and I. Glassman, "Gas Phase Oxidation of Isopropylbenzene at High Temperature," J. of Phys. Chem. 90, 508 (1986).
34. T.A. Litzinger, K. Brezinsky and I. Glassman, "Preliminary Experiments with 1-Methylnaphthalene near 1180K," Eastern States Meeting/The Combustion Institute Paper No. 68 (1985).
35. I. Glassman, "Physical and Chemical Effect in Soot Formation," Eastern States Meeting/The Combustion Institute Invited Paper D (1985).
36. K. Brezinsky, G.F. Linteris, T.A. Litzinger and I. Glassman, "High Temperature Oxidation of n-Alkyl Benzene," accepted for publication in 21st Symp. (Int'l.) on Combustion.
37. G.W. Sidebotham and I. Glassman, "Structure of Near and Slightly Sooting Inverse Diffusion Flames," accepted for presentation at 1986 Eastern States/The Combustion Institute Meeting.
38. F. Takahashi, F.L. Dryer and F.A. Williams, "Combustion Behavior of Free Boron Slurry Droplets," AFOSR TR-85-0559, May 1985.
39. F. Takahashi, F.L. Dryer and F.A. Williams, "Further Experiments on the Combustion Behavior of Free Boron Slurry Droplets," Eastern States Section: The Combustion Institute Meeting, Paper No. 19, November 1985.

40. F. Takahashi, F.L. Dryer and F.A. Williams, "Combustion Behavior of Free Boron Slurry Droplets," Twenty-First Symposium (Int'l.) on Combustion, The Combustion Institute, Pittsburgh, PA, 1986 (in press).
41. K. Brezinsky, "The High Temperature Oxidation of Aromatic Hydrocarbons," Prog. in Energy and Combust. Sci. 21, 1 (1986).
42. P. Antaki and F.A. Williams, "Transient Processes in a Non-Rigid Slurry Droplet During Liquid Vaporization and Combustion," Combustion Science and Technology, 49, 289 (1986).
43. P. Antaki and F.A. Williams, "Observations on the Combustion of Boron Slurry Droplets in Air," Combustion and Flame, to appear (1986).

#### IV. Professional Personnel and Graduate Students Theses

Prof. F.L. Dryer  
Prof. I. Glassman, Coordinator  
Prof. F.L. Williams  
Dr. K. Brezinsky  
Dr. F. Takahashi  
Dr. K. Saito

1. D.J. Hautman, "Pyrolysis and Oxidation Kinetic Mechanisms for Propane," Department of Mechanical and Aerospace Engineering, Ph.D. Thesis (1980).
2. J.A. Euchner, "A Study of the Oxidation of Toluene in a Flow Reactor," Department of Mechanical and Aerospace Engineering, M.S.E. Thesis (1980)
3. S.L. Murphy, "Pure and Oxidative Pyrolysis of Hydrocarbons in Relation to the Sooting Diffusion Flame," M.S.E. Thesis, Department of Mechanical and Aerospace Engineering, August 1982.
4. E.J. Burke, "A Study of the High Temperature Oxidation of 1,3-Butadiene," M.S.E. Thesis, Department of Mechanical and Aerospace Engineering, Princeton University, 1983.
5. P. Yaccarino, "Parametric Study of Sooting Diffusion Flames," Department of Mechanical and Aerospace Engineering, M.S.E. Thesis (1980).
6. Lt. K.E. van Teuren, "Sooting Characteristics of Liquid Pool Diffusion Flames," M.S.E. Thesis, Department of Mechanical and Aerospace Engineering, Princeton University (1978).
7. C. Venkat, "High Temperature Oxidation of Aromatic Hydrocarbons," Department of Chemical Engineering, M.S.E. Thesis (1981).
8. T. Litzinger, "The High Temperature Oxidation of Alkylated Aromatic Hydrocarbons," Department of Mechanical and Aerospace Engineering, Ph.D. Thesis (1985).
9. P. Antaki, "Studies of Slurry Droplet Combustion and Boron Particle Ignition," Department of Mechanical and Aerospace Engineering, Ph.D. Thesis (1985).

## V. Presentations - Seminars

### K. Brezinsky

"High Temperature Oxidation of n-Alkyl Benzene", 21st Symp. (Int'l.) on Comb., August 5, 1986, Munich, W. Germany

### I. Glassman

"Physical and Chemical Aspects of Soot Formation"

- Dept. of Mech. Eng., Rutgers U., Oct. 3, 1985
- Invited Lecture, Eastern States/The Combustion Institute Meeting, Nov. 5, 1985.
- Dept. of Mech. Eng., University of Florida, Jan. 30, 1986
- Research Center, Phillips Petroleum Co., Bartlesville, OK, Feb. 21, 1986.

### T.A. Litzinger

"Preliminary Experiments with n-Methylnaphthalene near 1180K", Eastern States Section/Combustion Institute Meeting, Nov. 5, 1985.

### F. Takahashi

"Further Experiments on the Combustion Behavior of Free Boron Slurry Droplets," Eastern States Section: The Combustion Institute Meeting, Paper No. 19, Philadelphia, PA, November 1985.

"Combustion Behavior of Free Boron Slurry Droplets," 21st Symp. (Int'l.) on Comb., August 5, 1986, Munich, W. Germany.

### F.A. Williams

"Observations on the Combustion of Boron Slurry Droplets in Air," presented at a Poster Session of the 21st International Symposium on Combustion, Munich, Germany, August 7, 1986.

## VI. Interaction With Other Laboratories

Discussions of environmental measurements with and lab visits by

Mr. S. Joshi  
Environs Division  
Tyndall AFB, FL

January and February, 1986

Correspondence and discussion with respect to aromaticity in current JP fuels with

Mr. Charles Martel, Wright-Patterson AFB, Ohio  
Mr. K. Holtby, Boeing Company  
Dr. P. Ames, McDonnell-Douglass  
Dr. D. Seery, United Technologies  
Mr. E. Lazburg, NASA LRC  
Mr. A. Cifone, NAPC, Trenton

(All in October, 1985)

END

1-87

DTIC